Laura A. Ayres

Constraints from magnetotellurics on the subsurface structure and emplacement of the Mourne Granites

2011

Earth Sciences, School of Geography, Earth & Environmental Sciences, University of Birmingham

870004
MSci Thesis

ABSTRACT

Studies of the Mourne granites, which form part of the British Palaeogene Igneous Province, have led to the development of granite emplacement models that invoke cauldron subsidence and more recently, based on magnetic-mineral fabric (AMS) data, a laccolithic emplacement. The key test between these models is in the subsurface distribution of granite. Cauldron subsidence predicts a deep stock of granite to >10 km depth, while laccolithic emplacement predicts a relatively shallow tabular granitic body extending towards a feeder zone in the south. The geology beneath and around the Mourne Mountains has been imaged along three 20 km long magnetotelluric (MT) profiles, to determine the spatial extent and geometry of the (electrically resistive) granites hosted in (more conductive) Silurian sedimentary rocks. In our 2-D MT models over the western and eastern magmatic centres, the bases of these granites are inferred to reach maximum depths of 6 km and 8 km respectively. A southerly-dipping resistor with a maximum thickness of about 4 km is observed to the south of the mountains. This suggests the presence of granite beneath surface country rocks and is consistent with the presence of a potential southerly feeder zone as predicted by the laccolithic emplacement model. The granites are inferred as being intruded as thin, tabular sheets *sensu* the laccolithic model, the eastern pluton in three or four sheets with a small amount of lopolithic, down floor movements also occurring. The western pluton as two, thinner laccolithic sheets with subsequent lopolithic movements.

This work was presented as a poster at the 54th Irish Geological Research Meeting, 18th – 20th Feb 2011.

TABLE OF CONTENTS

LIST OF FIGURES

1. AIM

The aim of this project is to discover the subsurface structure of the Mourne Mountains using three magnetotelluric profiles and to discuss possible emplacement mechanisms.

2. INTRODUCTION

2.1 Location and geology of the Mourne Mountains

The Mourne Mountains are located in County Down, Northern Ireland, on the south-east coast around 40 miles south of Belfast. They are part of the British/Irish Palaeogene Igneous Province and are composed of five distinct, intrusive, sub alkaline granitic members, G_1 to G_5 which are divided between an eastern and western centre. This granitic complex intruded into Silurian greywackes and shales (Hawick Group) at a high level, not reaching the surface, during the late stages of activity in the North Atlantic Tertiary Volcanic Province. Meighan *et al.* (1988) has determined an age of 56Ma for granites G_1 to G_4 using Rb-Sr isotopic measurements; G_5 was found to have a much younger age of 52Ma. Gamble *et al.* (1999) found U-Pb ages of 56.4 $\pm$ 1.4Ma for the G_1 granite and 55.3 $\pm$ 0.8Ma for the G_2 granite, in agreement with the Rb-Sr dates. Interestingly, Thompson *et al.* (1987) found a $^{40}Ar/^{39}Ar$ age for a basic dyke cross cutting G_5 of 55 $\pm$ 1.6 Ma and McCormick *et al.* (1993) states that unpublished $^{40}Ar/^{39}Ar$ data also don't rule out a 56Ma age for the G_5 granite. The four youngest granites, G_2 to G_5, were emplaced as a series of magmatic pulses. These have distinct textural characteristics which can be determined in the field and they represent a continuous, compositional series from olivine tholeiite, to intermediate through to acidic forming a sub-alkaline acid fractionation series, with G_1 being the most basic in composition; a hornblende-biotite syenogranite. Granite G_2 is a biotite granite, G_3 is an aplitic biotite syenogranite, G_4 is a biotite granite and G_5 is a biotite amphibole microgranite (Meighan *et al.* 1984; Cooper & Johnston 2004).

The mountains were first investigated by Richey (1927) who mapped the area and established the three granitic lithologies for the Eastern pluton (Figure 1). He also proposed the pulses of magma emplacement process and was one of the first authors to propose cauldron subsidence as an emplacement mechanism. Richey (1927) mapped the western pluton as one lithology, G_4, however the area has subsequently been remapped by Meighan (1979), Hood (1981), Gibson (1984) and Meighan *et al.* (1984). Meighan (1979) reclassified the western pluton into two lithologies G_4 and G_5, which were then further reclassified by Gibson (1984), with G_4 separated into fine, medium and coarse

areas and G_5 into mafic poor and mafic rich units. Hood (1981) also remapped the eastern pluton reclassifying some of Richey's (1927) G_1 'roof' as G_2 outer facies with a mafic variant. He also divided G_2 inner into a fine only, fine-medium and coarse areas and G_3 into mainly fine, medium-coarse and very coarse areas (Figure 2).

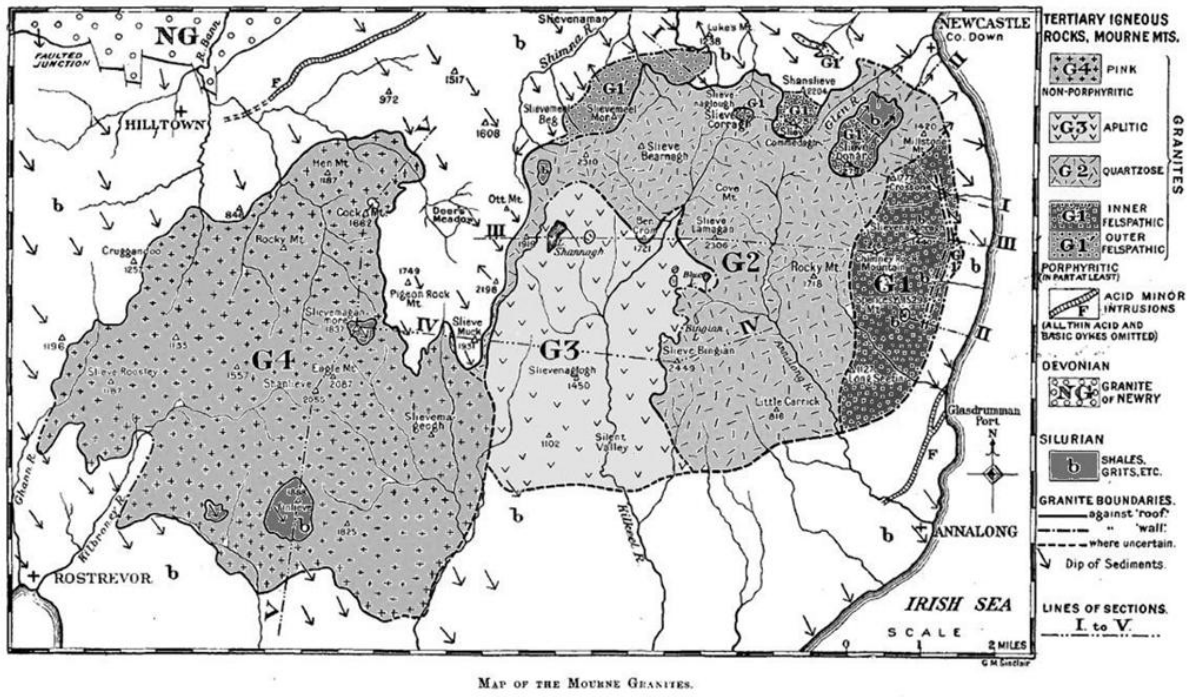

Figure 1, this is Richey's (1927) original map of the Mourne plutons with the three granitic lithologies in the east and one in the west. Taken from Richey (1927).

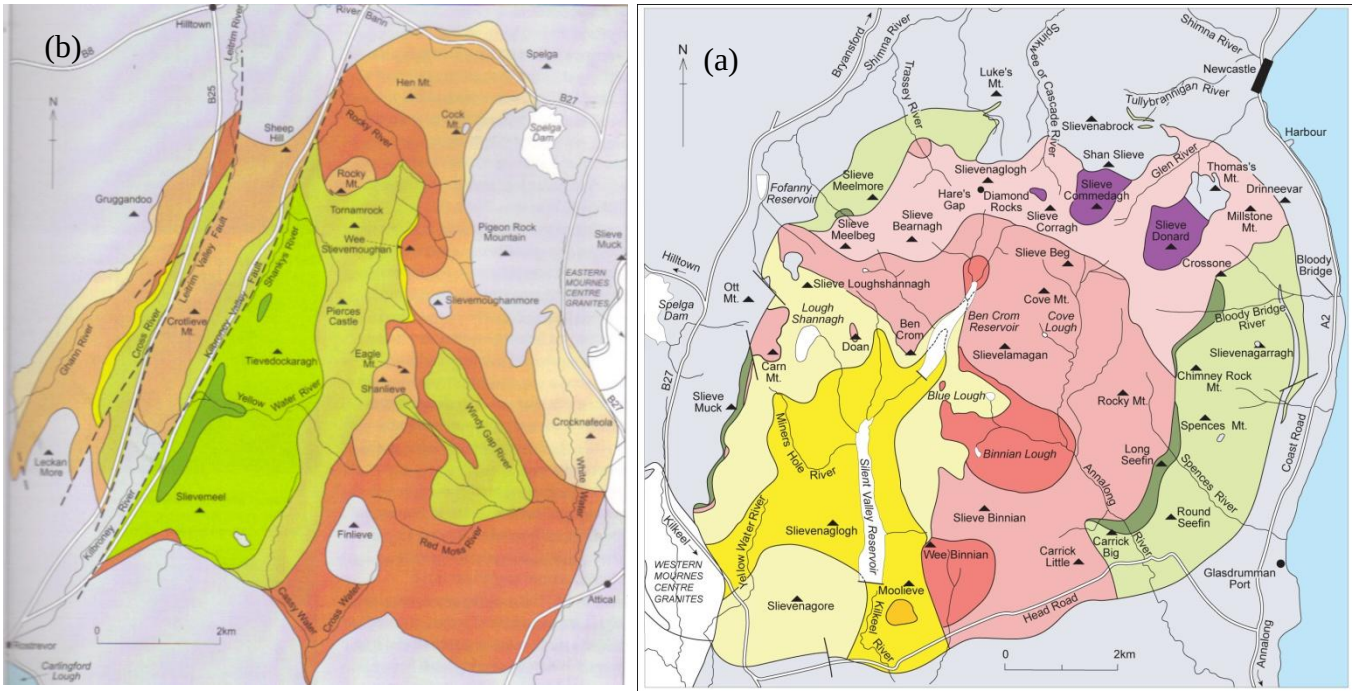

(c)

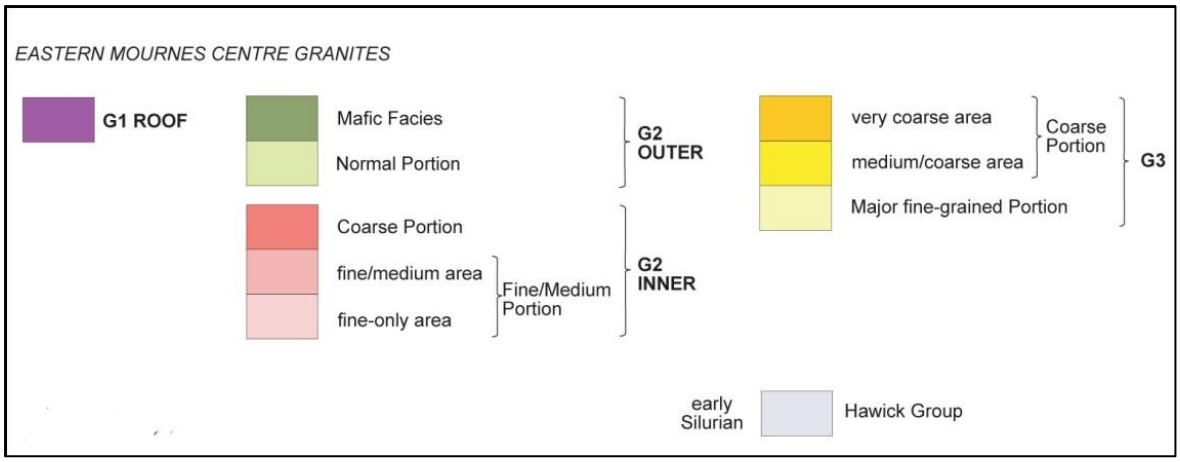

(d)

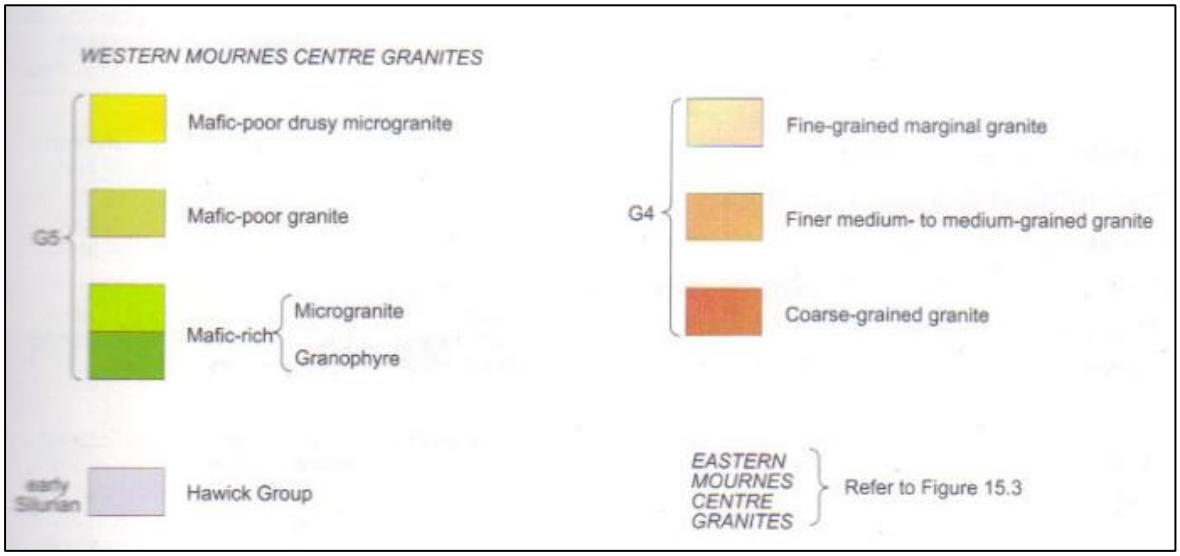

Figure 2, these maps (a) and (b) show the currently accepted geology of the area, after Hood (1981) and Gibson (1984) for the eastern and western plutons respectively. Areas from Richey's original maps have been altered with the major changes being the addition of G_5 in the western pluton and the re-classification of some of the G_1 'roof' to G_2 outer. Images (c) and (d) give the keys for the maps and the main features of the individual granite units. Maps and legends reproduced from Cooper & Johnston (2004).

2.2 Cauldron subsidence or laccolithic emplacement?

The long standing theory of granitic emplacement in this area is the cauldron subsidence mechanism, first proposed for the Mournes by Richey (1927), Figure 3. It was a novel theory at this time and had first been proposed for the Glen Coe intrusion in Scotland by Clough *et al.* (1909). The cauldron subsidence mechanism varies per intrusion, it depends on the nature of the intrusion itself and the surrounding country rocks, although, some general points remain similar; the members of the complex incline

inwards toward a common centre. The intrusions are arranged in continuous curves around the intrusion centres and the inner members of the complex dip more steeply (Anderson 1936). Originally it was assumed that the inner members would also be the youngest, however, recent work by Vigneresse (2004) has shown that the inner members can be either the older or the younger units. Anderson (1936) states that a cauldron subsidence intrusion is caused by a ring fracture forming at depth without reaching the surface. This extends down leaving the subsided rock hanging. The stresses which form this ring fracture may then form a cross fracture over the block of country rock causing the whole block to sink. The space this leaves will be filled with the ascending magma with the ring fracture acting as a channel. This will form the classic, steep sided, "bell-jar" intrusion. In rare cases the sides may be more vertical in inclination as reported for the Glen Coe caldera by Clough *et al.* (1909), however, they are most often outwardly inclined as reported by Richey (1927) for the Mournes (Clough *et al.* 1909; Richey 1927 and Anderson 1936).

Richey (1927) investigated and mapped the Eastern Mourne pluton and stated that the walls and slightly domed roofs are easily seen, that the three main eastern intrusions are arranged one within the other in a circular manner and that the steeply inclined or vertical walls do not suggest a laccolithic style of emplacement. These points, along with an absence of evidence for uplift, led Richey to believe that the cavity in which the granites now reside was created by a downward movement of the floor due to a cauldron subsidence emplacement mechanism, *sensu* Clough (1909).

Anderson (1936) numerically modelled the dynamics of cone-sheets, ring-dykes and cauldron subsidence mechanisms with an in depth section focussing on both the Mournes and Glen Coe, taking further the research of Richey (1927) and Clough *et al.* (1909). The Eastern Mourne pluton constitutes three successive intrusions where the first two partially surround the third with the boundary surfaces between the intrusions being vertical or steeply inclined. Anderson (1936) stated that when a certain height is reached, the steeply dipping surfaces bend over abruptly to a position which is nearly horizontal so that each member overlies and surrounds the previous. It is suggested that G_1 for the Mournes (the earliest intrusion) behaves similarly and so infilled a subterranean cauldron subsidence.

The cauldron subsidence mechanism is also thought to be applicable to the Western Mourne pluton but due to the present level of erosion only the flat 'roof' units are exposed (Cooper & Johnston 2004).

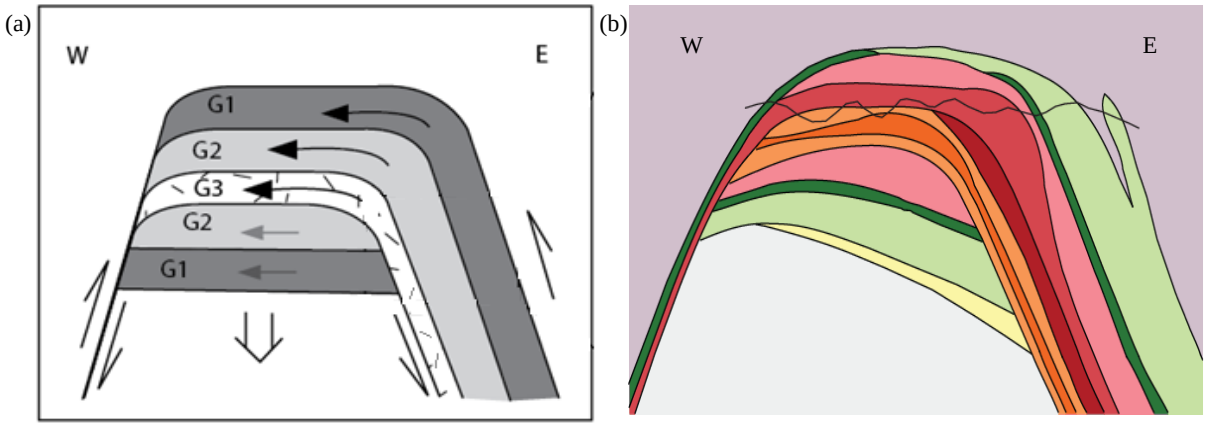

Figure 3, diagram (a) is Richey's (1927) cauldron subsidence model, showing diagrammatically his ideas for magma flow directions and the space creation mechanisms. Diagram (b) is the updated view of this classic model and gives the correct surface outcrop of all the 'new' divisions within the original granite units; this is taken from Cooper and Johnston (2004). Worth noting is the point that neither model has a vertical scale, suggesting the depths are fairly unconstrained.

The cauldron subsidence mechanism has remained the accepted emplacement mechanism since its proposal and hasn't been significantly challenged until Stevenson *et al.* (2007) used field data and evidence from an anisotropy of magnetic susceptibility (AMS) study to propose a laccolithic style of emplacement for the Eastern Mourne pluton (Figure 4). As mentioned above, some of Richey's (1927) original maps were altered by Meighan (1979), Hood (1981) and Gibson (1984) - the roof and wall geometry reported by Richey is no longer evident in these newer maps (Figures 1 and 2). The AMS data from Stevenson *et al.* (2007) showed that the internal and external contacts of the granites and the major and minor variants within the pluton are all gently dipping, not steeply, as proposed by the cauldron subsidence mechanism. Their AMS data also shows a strong linear component which would suggest that magma in-flowed from the SSW in a NNE direction, again not suggested by the cauldron subsidence model.

A similarly linear flow with gentle internal and external contacts has recently been found by Stevenson & Bennet (2011) who have suggested a similar laccolithic emplacement mechanism for the western pluton. A magma flow direction of NNE/SSW has also been reported (Figure 4).

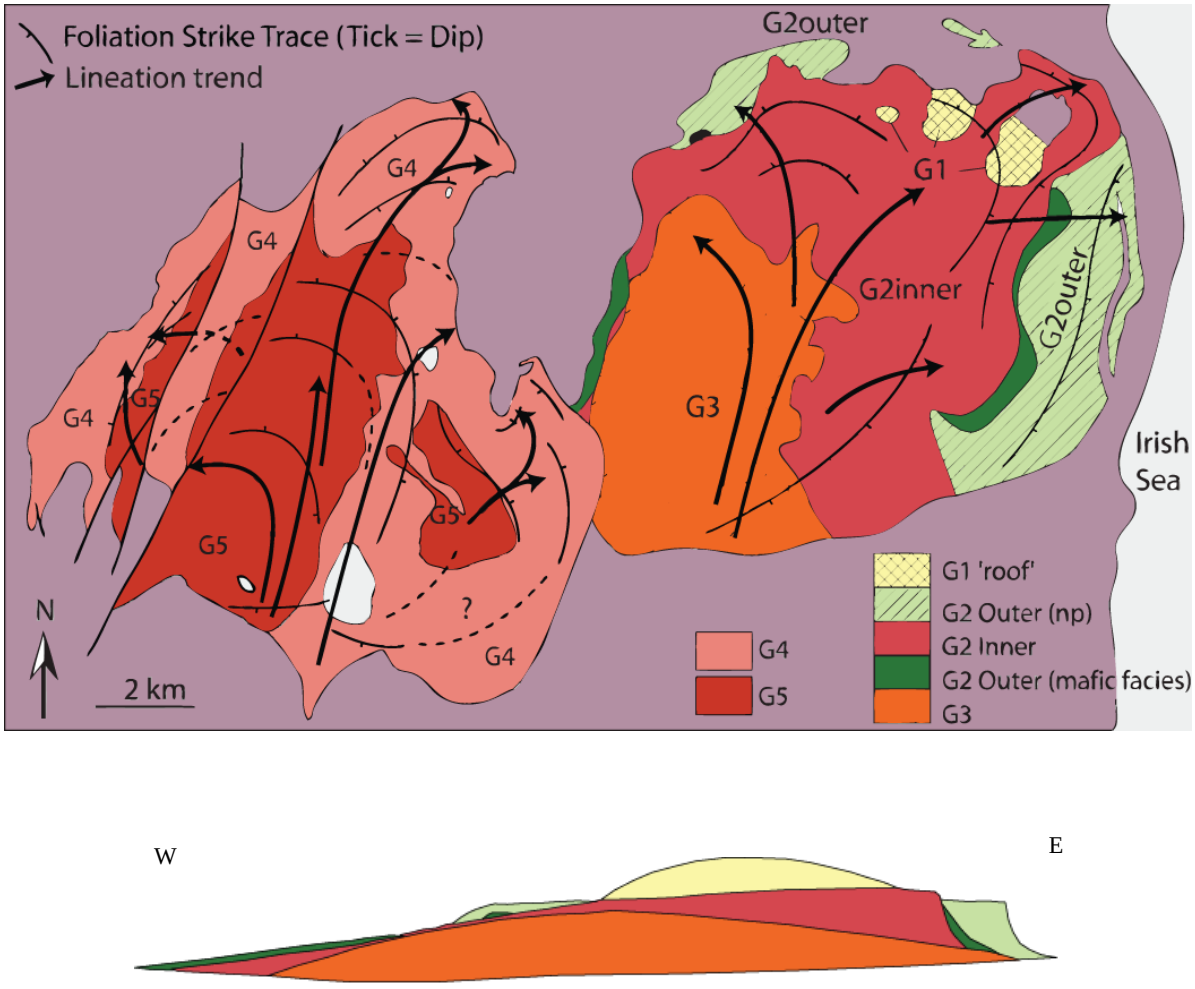

Figure 4, (a) Shows the AMS linear flow directions for both the eastern and western plutons as reported by Stevenson *et al.* (2007) and Stevenson & Bennet (2011). Image taken from Stevenson & Bennet (2011). (b) Shows Stevenson *et al's* (2007) proposed laccolithic model for the eastern pluton, taken from Stevenson *et al.* (2007).

The key test between these two models is the subsurface distribution of the granites; cauldron subsidence predicts a deep stock of granite extending from the surface to below 10km whereas the laccolithic model predicts a thin tabular sheet extending to the south. Stevenson *et al.* (2007) do not give a thickness for their model however, Cruden (1998) gives a general laccolith thickness of less than 3km, McNulty *et al.* (2000) state that the Mount Givens pluton has a thickness of around 5km and Bunger & Cruden

(2011) suggest a general thickness of between 15m and 2.5km.The subsurface distribution of the granite was tested using magnetotellurics.

2.3 Geochemical and geophysical evidence

Recently published gravity data (Figure 5) shows a continuous positive Bouguer gravity anomaly extending from the Slieve Gullion area to just offshore south of the Mournes (Reay 2004). The spatial location of the anomaly, in conjunction with the AMS fabrics suggests the magma might have travelled in a north/north easterly direction from a basic magma chamber (Stevenson *et al.* 2007). However, at present the gravity data have not been modelled to determine the extent and geometry of the anomalous body so a direct link cannot yet be well constrained.

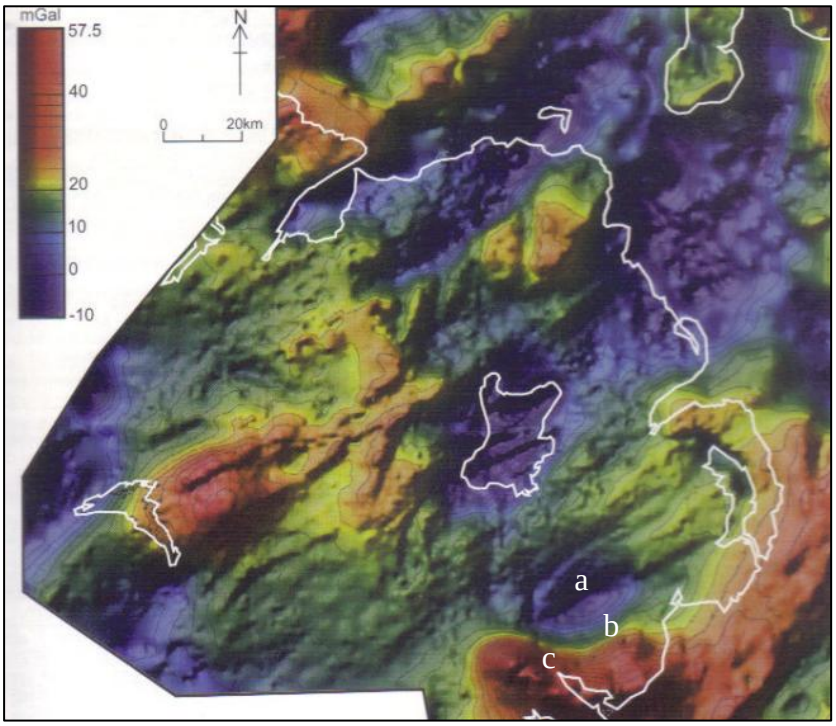

Figure 5, this image shows the gravity survey data from Reay (2004). Point a shows the location of the Newry granodiorites, b the location of the Mournes and c the positive anomaly. The Newry granodiorites show a negative anomaly as would be expected for an acidic intrusion; however the Mournes show no such anomaly. The positive anomaly (c) has been interpreted as an offshore magma source/feeder.

McCormick *et al.* (1993) completed an oxygen and hydrogen isotope study of the Mourne granites and concluded that the oxygen isotopic data rule out only partial melting of the country rocks as the origin of the granites. They also rule out an origin consisting of closed-system fractional crystallization of basaltic magma. This was concluded due to the enrichment of the units in $\delta^{18}O$, with G_2 having a value of

~+9.5‰, G_3 and G_4 with ~+9.0‰, and G_1 and G_5 are much lower with ~+7.5‰ and +7.5 to +8.5‰ respectively. It has been suggested (Taylor & Sheppard 1986) that for any value greater than $\delta^{18}O$ +7.5‰ the rock must have been derived from, or came into contact with, a material which is near to or was near to the earth's surface. This agrees with Meighan *et al's* (1988) $^{87}Sr/^{86}Sr$ data which doesn't suggest an isolated fractional crystallisation process or a solely crustal source either.

Meighan *et al.* (1988) collected Rb-Sr data over the Mourne complex and the surrounding area and found significant differences between initial $^{87}Sr/^{86}Sr$ ratios; G_1 (0.7129±2), G_2 (0.7109±3), G_3 (0.7104±6), and G_4 (0.7085 ± 17) (uncertainties 2σ) so the earliest unit has the highest ratio. This rules out a co-magmatic origin for the granites and the high radiogenic contents also suggest that extreme fractionation of a closed-system basaltic source can be excluded. The magmatic O isotopic data for the granites is much lower than the surrounding Lower Palaeozoic sediments suggesting that the magma could also not be a closed-system partial melt of this material. It is likely the granites are derived from one or more crustal sources with a substantial basaltic component derived from a partially melted mantle. Meighan *et al.* (1988) also suggest that a contamination from the northern Newry granodiorite igneous body could produce the values seen for the G_2 and G_3 granites, however, the G_1 (0.7129±2) value cannot be derived from the Newry granodiorite (Meighan *et al.*, 1988). This would suggest that the main feeder zone is unlikely to be located to the north of the Mournes as you would expect a greater contamination of G_1 from the Newry intrusion.

2.4 The Magnetotelluric method

Magnetotellurics (MT) is a passive geophysical exploration method. It measures the electromagnetic induction of the earth by utilising naturally occurring geomagnetic field variations (or the strength of fluctuations in the earth's natural electric and magnetic fields). This allows the conductivity structure of the earth from a few tens of metres down to hundreds of kilometres depth to be determined. The depth of penetration achieved by any individual recording, with a given sounding period, is dictated by the conductivity of the earth being measured. The transmission of electrical charge throughout the earth (or conductivity) occurs by free charge carriers within rocks and minerals. The resistivity structure obtained from the measurements can be related to the geology, temperature, pressure, physical/chemical state, porosity and permeability of the rocks below. For example, dry crystalline rocks can have resistivities exceeding 10^6 Ohm.m whereas seawater and graphite can be less than 1 Ohm.m. The naturally induced

electromagnetic fields within the earth have periods ranging from 10^{-4} to 10^{5}s and hence, a large range of penetration depths are possible with the MT method. In some cases depth's greater than 500km can be achieved. The majority of the earth's natural magnetic field is generated by fluid dynamic processes in the outer core, however, this is more or less constant with respect to the time periods relevant to AMT/MT. It is the shorter period variations in the magnetic field strength caused by the solar wind – magnetic storms- from sunspot activity which are used for MT (and lightning strikes for AMT) which induce the subsurface electrical currents taken advantage of in the MT methods. The largest external sources are those produced by magnetic storms; these can last for several days and give very good quality data. All these external fluctuations plummet between 5 and 1Hz producing an AMT 'dead band' which manifests as a poor data quality zone in most data sets (Figure 9); including the one obtained here. The MT dead band can vary but is located at the gap between energy from lightning storms and magnetic storms (Simpson & Bahr 2005).

The measured electrical and magnetic field variations at each site provide the MT response or impedance tensor. This is then numerically modelled to produce an electrical resistivity structure which can then be interpreted in geological terms. To image 2-D resistivity structures two orthogonal electrical fields are measured; the TE (Transverse electrical) and TM (Transverse magnetic) modes. The TE mode is parallel to electrical strike direction and the TM perpendicular. In a 1-D model either mode can be used, or an average between the two, as they should be equivalent. The greater the difference between the two modes relates to how strongly the structure is 2-D.

The MT method is based on several mathematical laws - and always obeys Maxwell's equations - including Faradays law which states that an electrical field (E) is induced by a changing magnetic field (B):

$$curl\ \mathrm{E} = -\partial \mathrm{B}/\partial \mathrm{t}$$

And Ohms law which states that a current density (J) will stay constant whilst the conductivity (σ) and the electric field (E) is variable:

$$\mathrm{J} = \sigma \mathrm{E}$$

This varying electric field can be related to geological structures due to charge build up at geological boundaries. Charge build up occurs when an electrical current passes through boundaries between layers of varying conductivity. When a geological layer is

more conductive a smaller electrical field will pass through it than through a layer with lower conductivity, resulting in charge build up at layer boundaries, this is manifested in the TM mode response.

MT is well suited for this investigation due to the differences in conductivity between the granites and the country rocks; granite on average has a resistivity of 10 000 Ohm.m and shales have a resistivity of on average 10 Ohm.m. (Figure 6), this is a clear contrast and should allow for reliable subsurface interpretations. MT is a relatively cheap option when compared with other geophysical methods or boreholes and is more eco-friendly and portable.

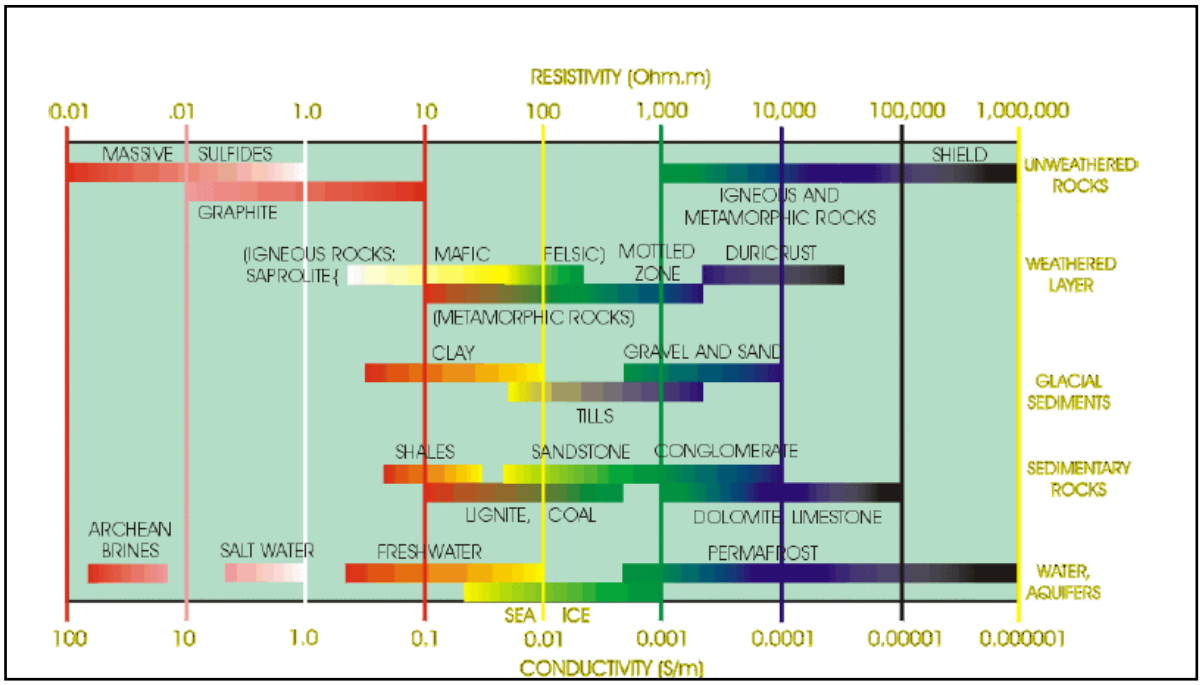

Figure 6, this image shows the general resistivities for common earth materials, it was used as a general guide during model interpretations. Jones, A.G. (2010) (Unpub. data).

3. METHODS

3.1 Location and layout of profiles

Three profiles were used to cover the area of interest; one over the eastern magmatic centre of the Mournes, one over the west and an east-west profile just south of the Mournes, with sites spaced around 1km apart on all profiles (Figure 7). Audiomagnetotellurics (AMT) was recorded at every site and MT at every other or every three sites; this is because MT measures longer periods and hence records deeper into the earth. So these sites can be spaced further apart to give the same resolution of data.

The sites along the profile must fulfil a certain criteria they must:

1. be far from external noise e.g. electric fences
2. be away from residential dwellings
3. on as flat topography as possible
4. be around 1km from the sites on either side along the profile
5. be a large enough size to include the 50m electrical lines

Permissions were obtained from authorities and private land owners before commencement of the survey.

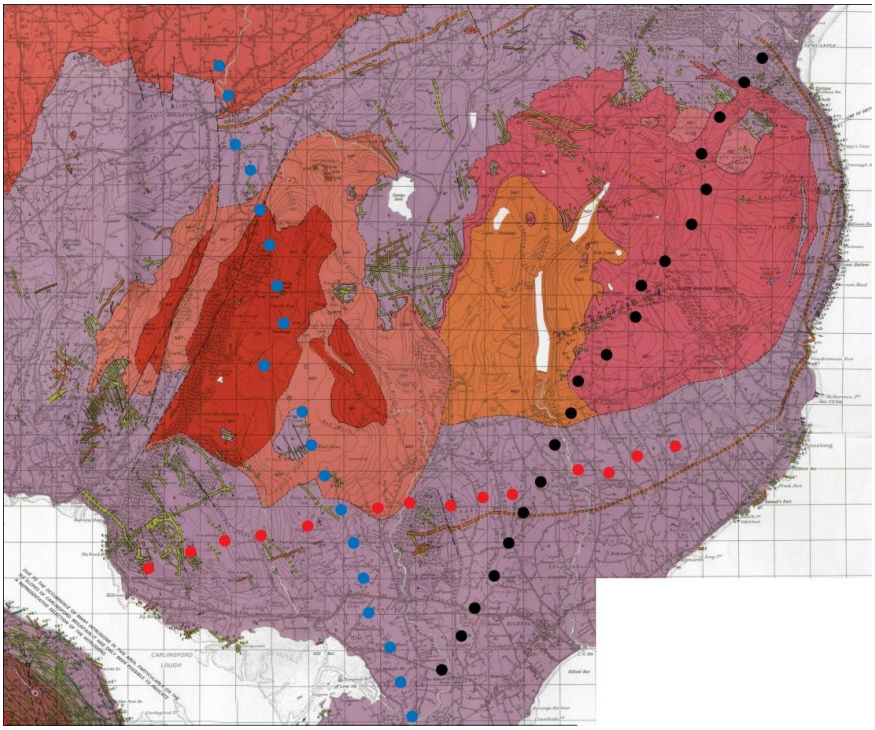

Figure 7, showing the geographical and geological locations of the individual sites. Black dots = EMC profile, blue dots = WMC profile and red dots = SLA profile. Re-produced from The Geological Survey of Northern Ireland, 1978.

N.B The data were collected by both myself and Chris Yeomans among many others, however I have processed, edited and modelled the EMC line and the methods referred to here relate to this profile. Chris has done the same for the WMC line. We have shared our final models for separate interpretations. The SLA line has kindly been processed and edited by Dr. Mark Muller and modelled by myself and Chris separately.

3.2 Data collection

Coil calibration

To ensure the equipment is functioning properly before recording commences the magnetometer coils are connected to the MTU boxes and set to calibrate for two hours. This calibrates the frequency response of the coils and produces a curve of the range of frequencies the coils are recording.

Site setup

A site consists of five non-polarizing electrodes; one located at the centre point of the site; and then one each at directly north, south, east and west, 25m from the central electrode. 25m should give a good signal to noise ratio however, if the site only allows a smaller spacing this ratio will decrease. The north and south electrodes compose the Ex line and the east-west electrodes the Ey line. The electrodes are used to measure the earth's electric field variation. They are buried in the ground to maintain a constant temperature and watered to ensure a good conductive connection with the soils. Three types of electrode were used during this survey; copper sulphate electrodes, lead chloride electrodes and metal stake electrodes which are watered with $CuSo_4$ solution and salt water respectively and the stakes hammered into the ground.

For recording AMT data MTC30 coils were used and for MT data MTC50 coils were used together with a Phoenix MTU-5 recording box. For an AMT site three coils were used; two were laid horizontally and perpendicularly, one precisely in line with north/south and the other in line with east/west. These two coils are placed with the wired ends to the south and west, to ensure correct polarity. The north/south coil is the Hx coil and the east/west the Hy coil, these are buried around 10cm into the ground. The third coil records the vertical magnetic field (Hz); it is placed vertically into the ground as far as possible and within a separate quadrant to avoid interference with the horizontal magnetometers, Figure 8. This vertical coil wasn't used for MT sites as logistically the coils are too large to get a significant length of it buried in the ground.

The coils and electrodes are connected by wires to the MTU-5 box which is also connected to a 12v battery and GPS receiver. This allows the sites which are installed on the same day to be recorded precisely in synchronisation, enabling remote referencing to be completed after acquisition of the data. The box is connected to a laptop on which the MTU parameter table is completed and then uploaded including information such as e-line lengths, coil numbers and recording start and end dates/times. The table also gives information such as latitude/longitude and internal battery voltages. When this table is uploaded the box will begin acquisition at the specified time.

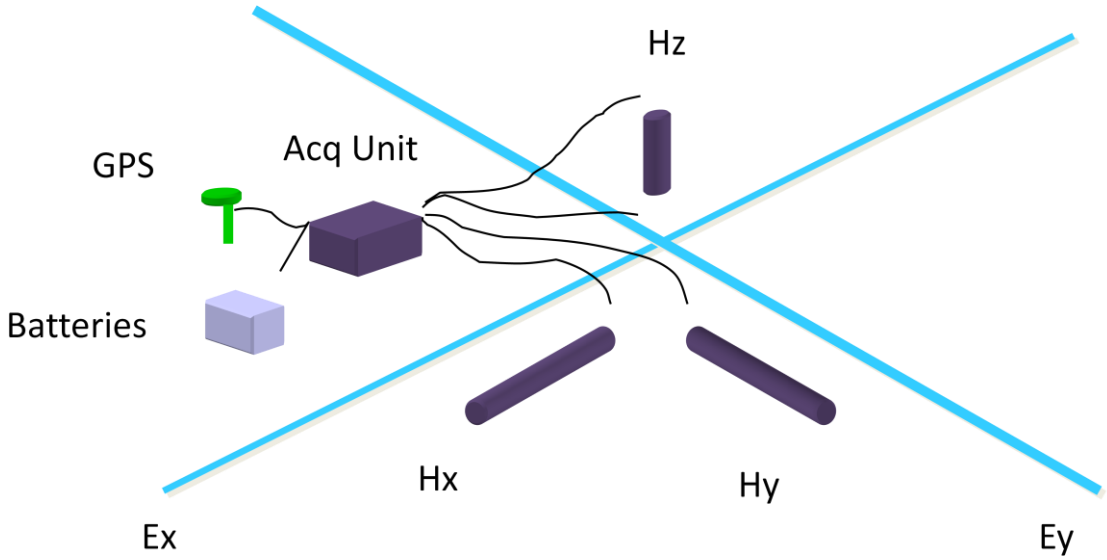

Figure 8, this is a schematic diagram of the site set up, although this would be a site where only AMT was being recorded, with a joint AMT and MT site there would be two more coils in a separate quadrant with a separate acquisition unit, GPS and battery. The Ex and Ey lines are aimed to be 50m at each site, however, the figure is not to scale. Jones, A.G. (2010) (Unpub. data).

3.3 Data analysis

Processing

The data are collected the following day and checked for noise by viewing in program syncTSV; if it is of acceptable quality, the data is saved on the laptop and two external hard drives. These data files acquired in the field are in time series format which are then opened with the program SSMT 2000 and converted to the frequency domain with a Fourier transform. Once the data are converted to frequency, local processing with respect to the magnetic field is completed to derive the MT response; it most cases a

remote reference site can also be processed alongside if the recording times are coincident; this process removes regional noise and so is more desirable than local processing. In our case three or four sites were usually recorded on the same night so, for example, Site 1 would be processed locally and then with each site that was recorded on that day i.e. Sites 1 and 2, Sites 1 and 4, Sites 1 and 6 providing four similar responses, the best of which would then be selected for editing. The processing method produces files in which each frequency has been divided into a specified number of partial solutions, normally 100. These partial solutions display the data in terms of phase and apparent resistivity of the MT response, Figure 9.

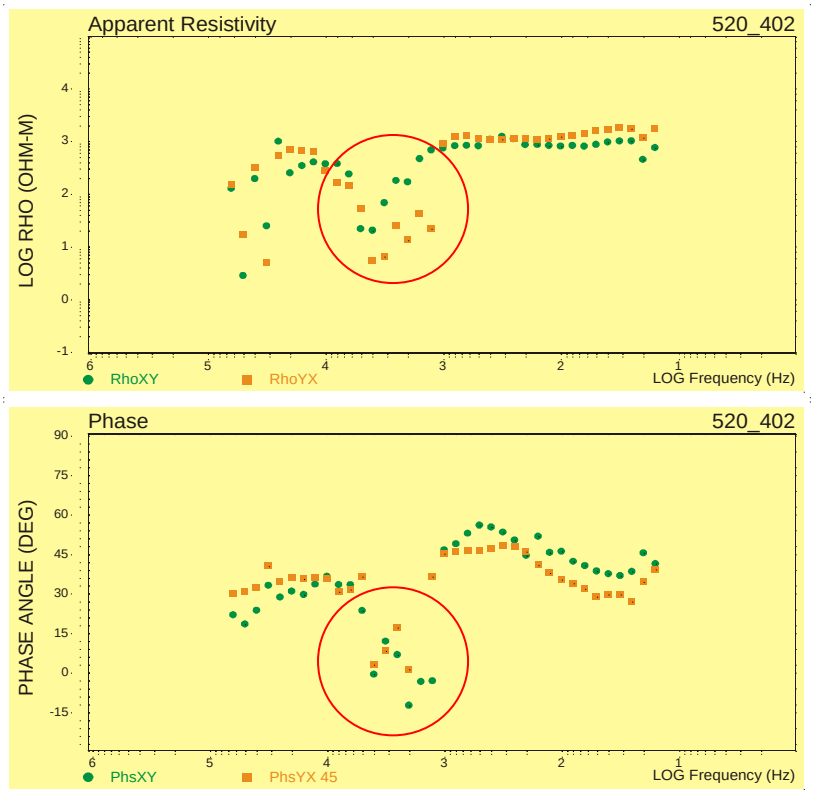

Figure 9, this image shows an example of un-edited data, the top image relating to apparent resistivity and the bottom to the phases. The red circle also shows an example of the MT 'dead-band'. Jones, A.G. (2010) (Unpub. data).

The topographic gradient of the sites is also important; ideally an MT site is located on flat topography but as the sites also need to be spaced evenly along a profile it is not always possible; in this case the area with the least elevation difference between electrodes is favoured. The greatest elevation difference at any particular site was 10m. Using trigonometry the new horizontal e-line length could be calculated, the resulting difference in length was 1m. The calculated difference in e-line length is that between

the actual horizontal distance – which is needed for accurate processing- and the along-surface distance measured between the electrodes. The data were then reprocessed with this new e-line length to asses any difference in the computed MT response. When both sets of data were compared, there was no apparent difference and considering the maximum difference in e-line length amounted to 1m it was decided that reprocessing of all sites with elevation differences was not necessary.

Editing

The files created by SSMT 2000 are then opened with the program MTeditor; the favourite response of all the possible remote reference options is chosen, usually the one with the least noise (See Appendix 1). This site then edited; all of the contributions which are clearly from other sources e.g. electric fences and are not a natural response from the earth are removed as far as possible, Figure 10. This is completed for every AMT and MT site. When editing is completed each site is then exported as an .edi file.

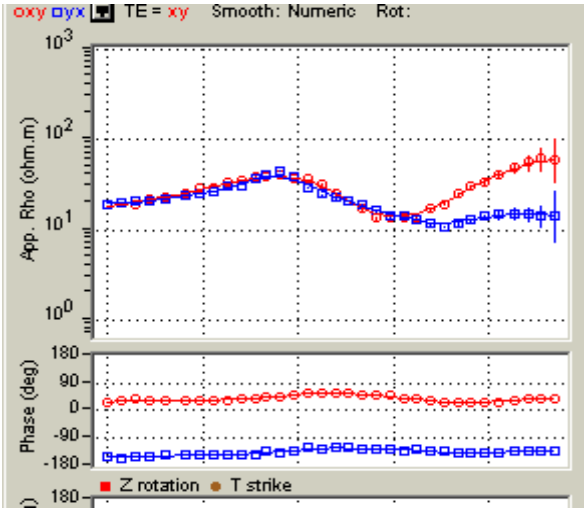

Figure 10, this shows some of the edited EMC line data, it can be seen that all of the erroneous data points have been removed and the data is now ready for modelling.

Preliminary 1D modelling

The .edi files are then be imported into WinGlink. Here the station geographic coordinates are projected using a transverse Mercator system using the WGS 1984 datum and spheroid system. The station data are linked together on a profile line and then each site undergoes D+ smoothing in which a curve is fit through the data taking into account both phases and both apparent resistivities. The D+ smoothing ensures that the apparent resistivities and phases are mathematically consistent. If they are

inconsistent, which may happen in the presence of noise or 3D geological structure, the data must be rejected and so is edited out before modelling. Each site then goes through a 1D inversion, firstly with a smooth Occam model which goes through several iterations to find a model to fit the recorded data and secondly a simple layered model is fit to the observed data points. These models can then be viewed as a cross section with the resistivity's displayed with a colour palette with dark blues showing highly resistive areas and red conductive areas, Figure 11.

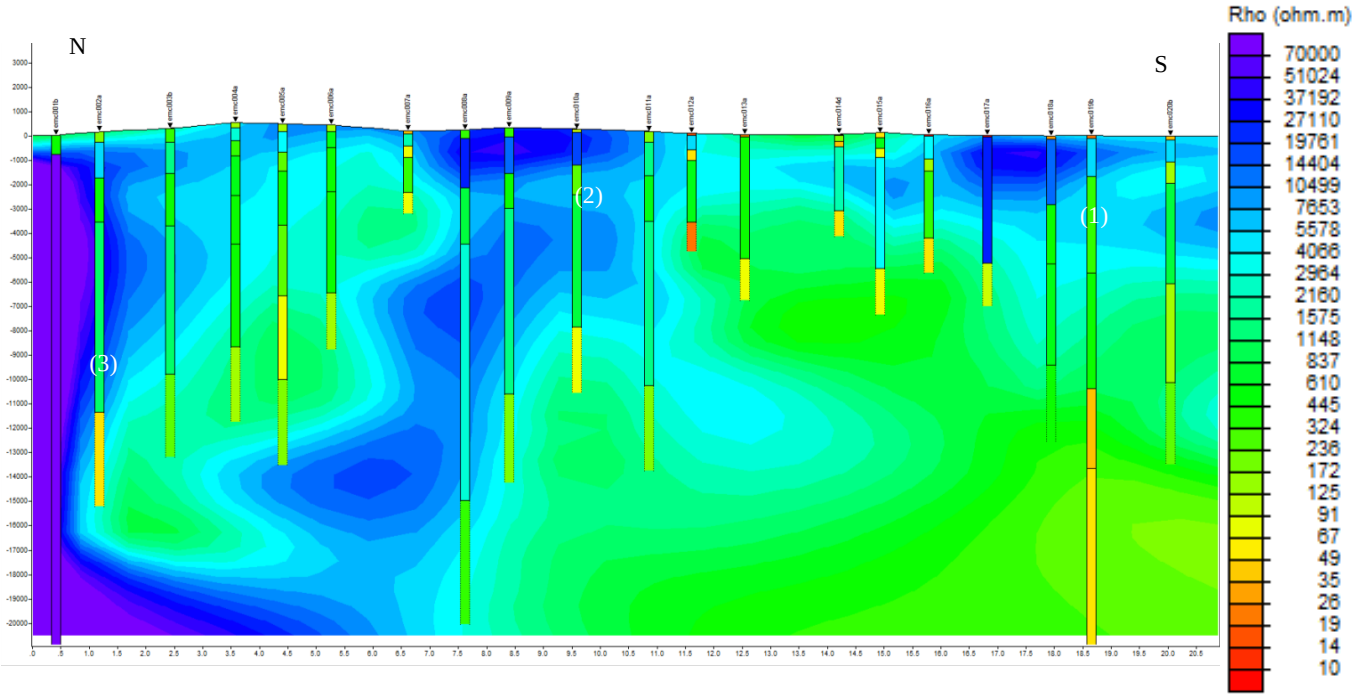

Figure 11, this is the EMC line magnetic north, AMT data only, 1D profile, the model extends down to 20km depth. Several resistive areas can be seen; one to the south of the profile (1), one at the southern end of the granite outcrop at surface (2) and a large area in the north (3). It should be remembered when looking at 1D models that and 2D or 3D geological features cannot be shown and that any anomalous areas (3) are due to this effect. It also must be remembered that the lines underneath each site represent the depth of penetration of the data and so anything below these is unconstrained and should be ignored.

Conversion of data to true north

When in the field the data are collected aligned to magnetic north using a compass; however magnetic north is not a convenient coordinate reference frame as it varies spatially from place to place and so the data is re-orientated to true north. This is done using program edi2edi.pl where the start-up file table (for that site) is entered and the .edi file name. The program uses the latitudes and longitudes from the start-up table and the IGRF (International Geomagnetic Reference Field) model to calculate the degrees difference between magnetic north and true north for that location, i.e. the magnetic inclination. For most sites it was around 4˚.

Merging of AMT and MT

At the sites where both AMT and MT were recorded, their frequency ranges overlap and hence so do some data points, therefore the data are merged at the point which gives the best of both sets of data and cuts out noise at the boundaries of their frequency range. The merge is done by converting both AMT and MT files from .edi to .dat with the program edi2j. The individual sites can then be plotted on top of one another, using program mtplot, to analyse the best overlap point. When a particular period is chosen, the two files are entered into the program mtmerge, where the two files are merged at the specified point and all overlapping data points are deleted. This process merges all of the data elements; apparent resistivity, phase and tipper. Unfortunately, as we only recorded tipper data at AMT sites, the new merged sites have some good tipper data in the overlapping range deleted and replaced with "false" MT tipper data. To resolve this issue, any AMT tipper data which were cut out were then re-entered manually using a text editor and the false MT data deleted.

Remodelling

These new files were imported back into WinGlink and again modelled in 1D, Figure 12.

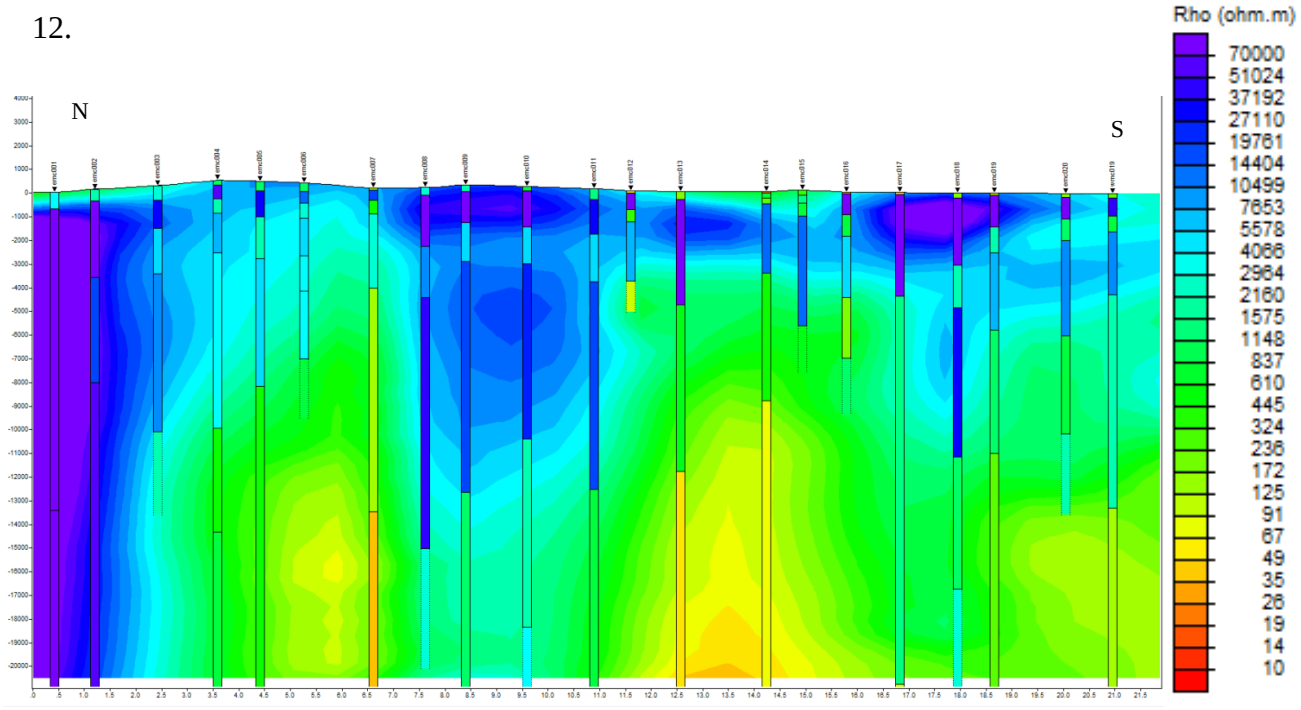

Figure 12, this is the EMC line true north, AMT data merged with MT data, 1D profile. This figure is quite similar to Figure 11; however, the base of the model is much better constrained due to the addition of the MT data. This model shows a continuous, thin, tabular resistor throughout the length of the profile with a deeper area underneath the surface outcrops. The model extends down again to 20Km.

In a 1D response the same field of currents are measured in two perpendicular directions (XY and YX) as there is no charge build-up because the 1D model assumes a simple layered geology. In a 2D model the XY and YX modes are polarised into two fully decoupled current systems (TE and TM) because of the charge build-up at boundaries affecting the TM mode. Whereas in a 3D model the charge build up will affect both XY and YX. The preliminary models and soundings were assessed for each site to determine to what extent they represented 1D or 2D subsurface structures. It was decided that approximately half of the sites had responses due to a 2D structure and the other half 1D. In this case, a 2D model is needed to model the structure accurately as 1D sites can be successfully modelled on a 2D model.

Strike analysis

To begin creating a 2D model the data have to be rotated (or decomposed) so that they are parallel and perpendicular to electrical strike direction, otherwise the resulting model is unreliable. (See chapter 2.4)

Firstly the program strike1 was used; this assesses the sensitivity of each individual site to all possible electrical azimuth directions and creates a colour scaled plot (Figure 13). The code for the program strike is based on the method of Groom and Bailey (1989) as implemented by McNeice & Jones (2001). The Groom and Bailey (1989) method is used to analyse the data to identify the best electrical strike direction. This colour scaled plot relates to the RMS error between the observed MT data and the Groom and Bailey (1989) 'model' for a particular strike azimuth. Where the azimuth is appropriate to the subsurface structure the Groom and Bailey (1989) 'model' fits well and the RMS error is small. In the scale the blue areas relate to the strike direction with the lowest errors. Some sites are all or mostly blue, indicative of a 1D structure in which any strike direction is reliable for that site (See Chapter 2.4). These plots were completed for the following frequencies:

1. 1000-100Hz
2. 100-10Hz
3. 10Hz-1s
4. 1-10s
5. 1000-10Hz

And the following depths:

1. 0-500m.
2. 500-1500m
3. 1500-2500m

4. 2500-5000m
5. 5000-10000m
6. 500-5000m
7. 5000-10000m

Although the data extend deeper than this depth range the area of interest is surface to 10000m.

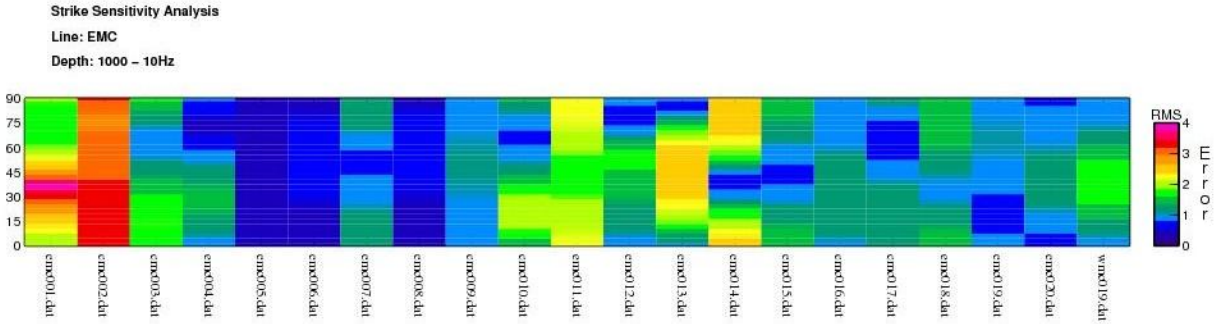

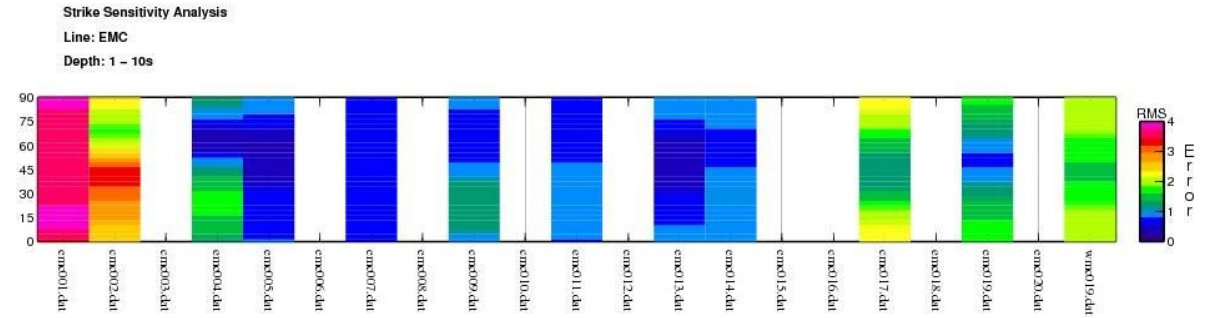

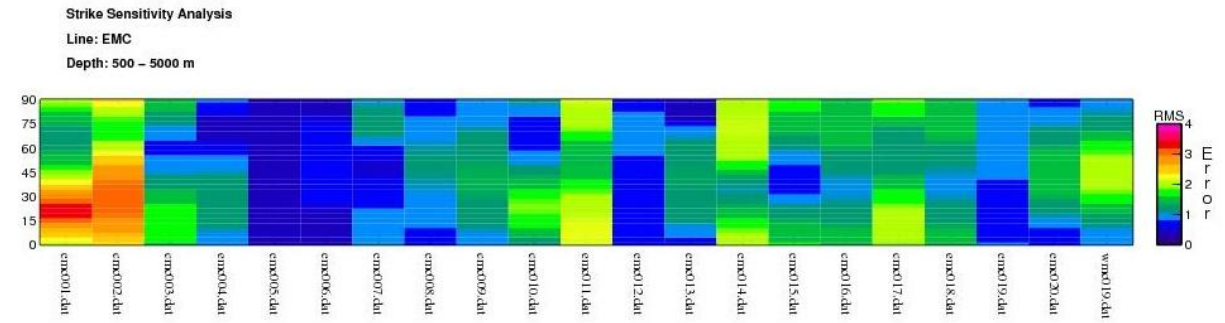

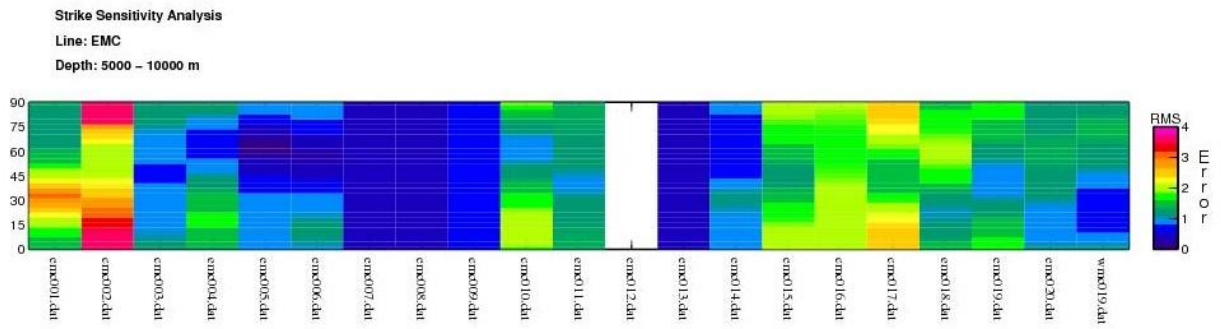

Figure 13, these four figures show the strike analysis over several frequency and depth ranges for the EMC line. The scale at the left hand side of each relates to potential azimuths. The RMS error scale bars on the right give the scale for the visual representation of the amount of error for any individual direction. The completely blue sites relates to the fact that the geology below them is 1D and so they would be happy with any strike direction. The sites which are blank have no data for the whole depth or frequency range imaged. These plots among others and alongside a strike analysis output helped decide the electrical strike directions for each profile. Full plots, Appendix 3.

To construct a 2D model, a profile is firstly required. In the 1D model case, the profile used ran along the line of sites, however in a 2D model it is required that the profile be constructed perpendicular to the electrical strike direction (and therefore parallel to the TM mode direction) to satisfy the physics of electrical current flow in a 2D medium. Therefore one single electrical strike direction is ideally needed for the whole profile and for all sites. The program strike 25x75 was used to find the best possible strike direction, taking every site into account over a certain depth or frequency range. It provides a single strike direction for all sites and the confidence level that quantifies the extent to which the data can be reliably modelled as 2D. Strike 25x75 was implemented for every frequency and depth range mentioned above.

Before a final strike direction was decided on, polar diagrams and tipper strike diagrams (Appendix 2) were also produced for every mid-point in the frequency ranges mentioned above.

Using all of this data together, final strike directions of 72˚ for EMC, 34˚ for WMC and 30˚ for SLA were decided upon. The data can then be decomposed (‘rotated’); this was completed using the Groom and Bailey (1989) decomposition approach. Groom and Bailey decomposition not only rotates the data but also uses a distortion matrix which removes galvanic (electrical) distortions (caused by small, poorly resolved conductors or resistors). This process rotates the data to a given azimuth and provides an RMS error (Root Mean Square difference) for each MT data point that reflects how well the data

match the chosen strike direction and the assumption that the subsurface structure is 2D. These RMS error values then get included within the output data file as “new” data errors. The Groom and Bailey (1989) method outputs files in g.dat format and for them to be re-imported into WinGlink they are converted back to .edi file format.

Groom and Bailey decomposition doesn’t rotate the tipper data, so these data are rotated separately and then merged back into the file. However as the tipper data is only rotated there is no distortion matrix implemented and so whilst the apparent resistivities and phases are assigned new data errors after Groom and Bailey decomposition, the tipper data retain their “original” observational errors that do not directly reflect the extent to which they satisfy a 2D model. After this decomposition method a new 1D model is again created at the new strike directions, Figure 14.

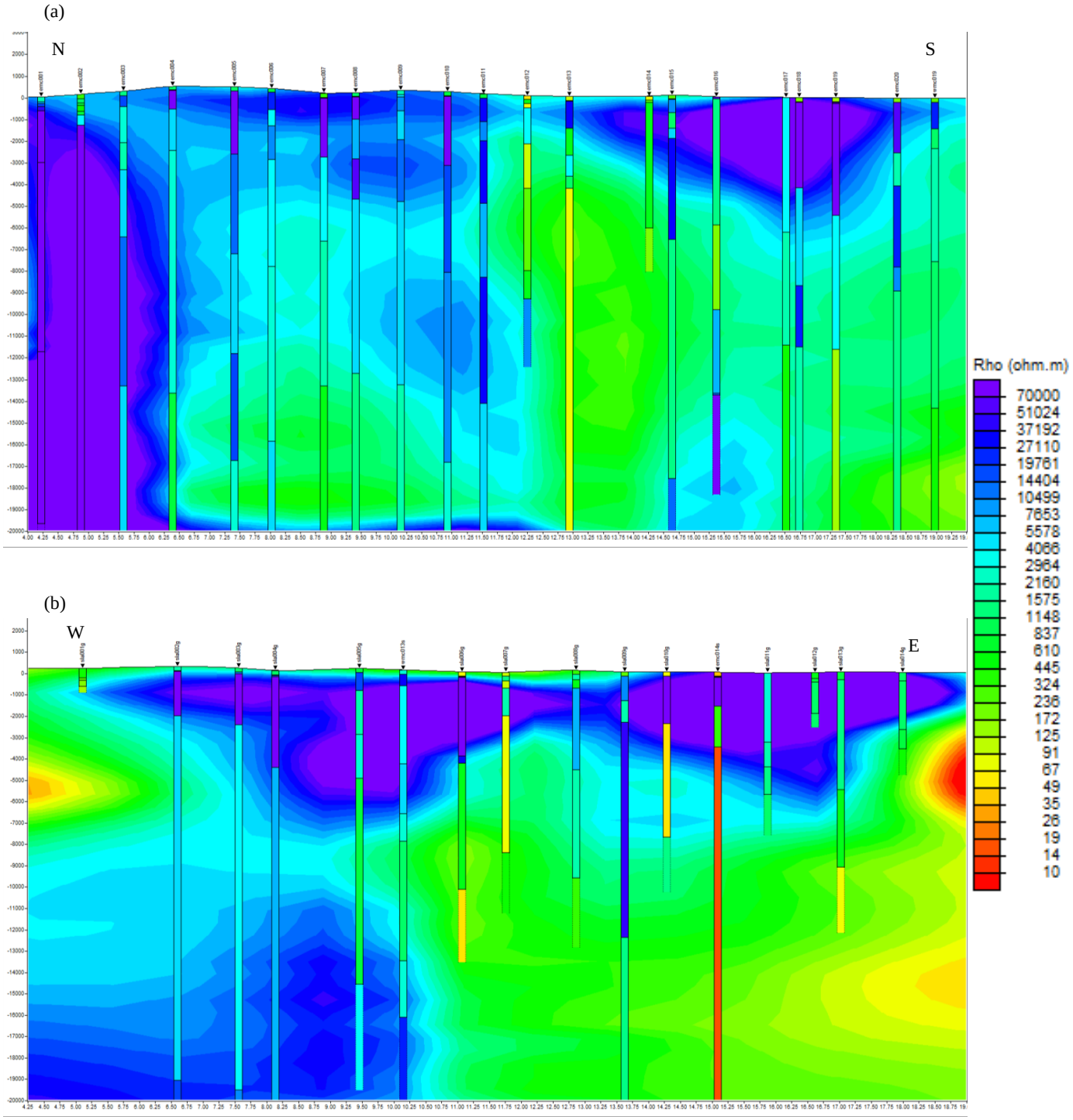

Figure 14, (a) shows the 72° 1D profile for the EMC line. The geometry of the resistive bodies is not much changed from the previous models; however, the resistivity values have increased as shown by the increased purple and dark blue areas. (b) Shows the 30° 1D profile for the SLA line, from this model, two distinct resistive areas can be seen corresponding to the eastern and western plutons. The resistive area in the east appears to extend to the surface; however, we know this is not the case. What has to be remembered is that similar to the penetration depth of the sites, they also have a starting penetration depth; most sites can't record anything above a few hundred metres. This does suggest, however, that the Silurian shale cover must be thin, less than a few hundred metres.

3.4 2D inversion

In the 2D inversion modelling that follows, data with large errors (i.e. data that poorly match the 2D assumption) are systematically down weighted, while data with small errors are more strongly weighted. The approach ensures that a 2D subsurface model is found that satisfies the MT data only to the extent to which they are 2D. To begin a 2D inversion, a grid mesh must be designed. A standard coarse mesh and a standard fine mesh were created within WinGlink and a forward model was run to test the responses of a 100 Ohm.m half space. The responses are assessed for how closely they produced apparent resistivities equal to 100 Ohm.m and phases equal to 45˚, deviations from this suggest that the mesh is not accurately representing the topography/shape of the modelled area. Deviations were found in both meshes, so a middle ground was produced with a finer mesh closer to the sites and increasing in size outwards. This had the smallest deviations.

The skin depth for the model also needed to be calculated and considered when creating the mesh. Two different equations can be used; skin depth or Bostick depth:

Skin Depth - $\delta = \sqrt{\frac{T\rho}{\pi\mu^o}}$ Bostick Depth - $h = \sqrt{\frac{T\rho}{2\pi\mu^o}}$

Where T = period in seconds, ρ = resistivity in Ohm.m and μ^o = magnetic permeability of vacuum= $4\pi \times 10^{-7}$ H/m.

Resistivity (Ohm.m)	Frequency (Hz)	Skin Depth	Bostick Depth
100	1000	159.06	112.58
100	100	503	356
1000	1000	503	356
1000	100	1590.63	1125.77

These calculated depths relate to the depth or lateral distance to which the data frequencies are sensitive – effectively the depth or distance projected out from the site in a semi-circle. Within the mesh, the MT sites should not be less than this distance from a corner in the model. This poses a particular problem for our model, as the expected granitic lithologies will have resistivities of at least 1000 Ohm.m and with the

steep topography present at the surface it is not possible to keep the sites away from the corners by this distance. This could therefore affect both the model and the real data.

For a 100 Ohm.m half space starting model, the models apparent resistivity responses seen in the TM and TE modes should be a flat line at 100Ohm.m. However deviations were seen in the TM mode, TM is the mode in which currents travel perpendicular to the geoelectrical strike, along the profile line; the deviations are thought to relate to topographical effects (Figure 15). The topographic effects may be contained in the actual data where the electrical and magnetic fields could get distorted by the steepness of the hills or the distortion could be due to the misrepresentation of the real topography by the model. The TE mode is unaffected by topography in the forward responses as these currents travel perpendicular to the TM mode and a 2D model assumes an infinite continuum of the model in that direction (i.e. perpendicular to the profile). This may pose a further problem as the real TE mode data may also contain topographic effects which cannot be accounted for by the 2D model and may end up being portrayed as spurious geological features in the model. The potential effect of topography on the TE mode would need to be tested using a 3D forward model which incorporates a 3D DTM.

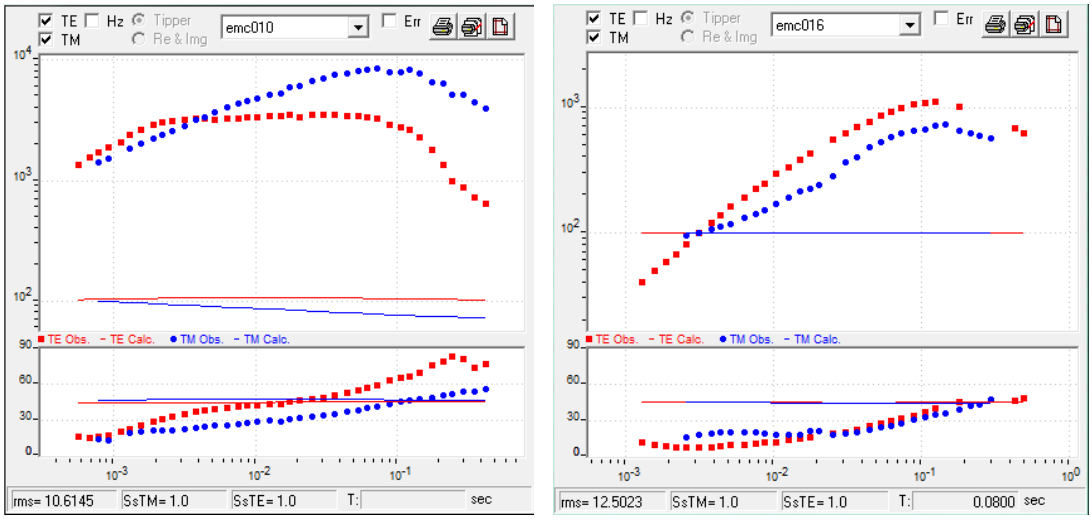

Figure 15, these two images show data from the EMC line, the red and blue dots show the actual station data. The straight lines represent the response of the starting mesh to a 100 Ohm.m half-space. We would expect to see a straight line at 100Ohm.m for apparent resistivities and a straight line at 45° for the phase. The image on the left shows station emc016 and a perfect response, however, the image on the left is from site emc010 and is an example of the potential 'topographic effect' as seen in both the eastern and western profiles. The reason site emc016 does not show this effect is assumed to be because it lies on fairly flat ground, this effect was only seen in the sites over and around the edges of the mountains, hence, its name the 'topographic effect'. It can be seen that its effect on the data at some sites is quite pronounced.

Any possible effects of Carlingford Loch just south of the eastern and western profiles and west of the southern profile and the Irish sea to the east of the southern profile needs to be tested, as saltwater has a resistivity of around 1.0 Ohm.m, which is significantly different to the geological features concerned. This "coastal effect" was tested by taking the standard 100 Ohm.m model and computing a forward response, saving these responses as station data (on a copied data set) then adding in cells to replicate the size and shape of the loch and fixing these cells at 1.0 Ohm.m. Then running the forward response with the sea included, to test the effect it would have whilst isolating any other possible effects; the coastal effect was deemed significant and so the Loch and sea were included in the final models, Figure 16.

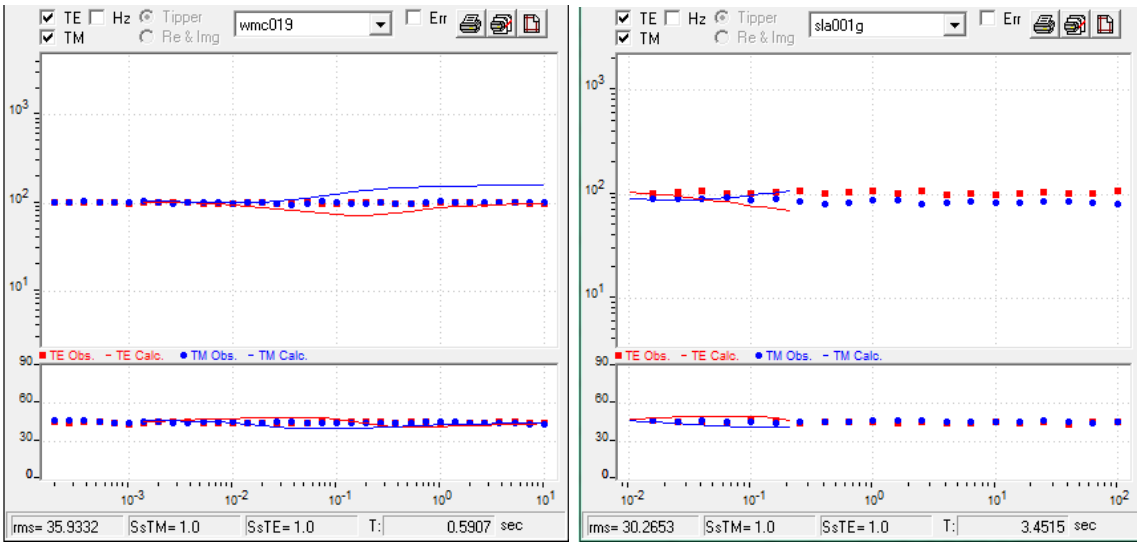

Figure 16, these two images show the test results for the effect of the proximal seawater on our data. The left image relates to the EMC line and the right to the SLA line, these images show clearly that the seawater has an effect on our data, and so, it was accurately represented on all final models for each profile to remove the deviation seen here.

The Tau (τ) or 'smoothing' factor used was 3 this was determined using a 'trade-off' curve between Tau value and RMS (Root Mean Square) error (the error between the observed and modelled MT responses), see Figure 17. Tau values of 50, 25, 12, 6, 3, 1, 0.5 and 0.1 were tested using the same starting model and identical inversion parameters and running "phase only" inversions for 99 iterations. Their respective RMS errors were recorded and plotted.

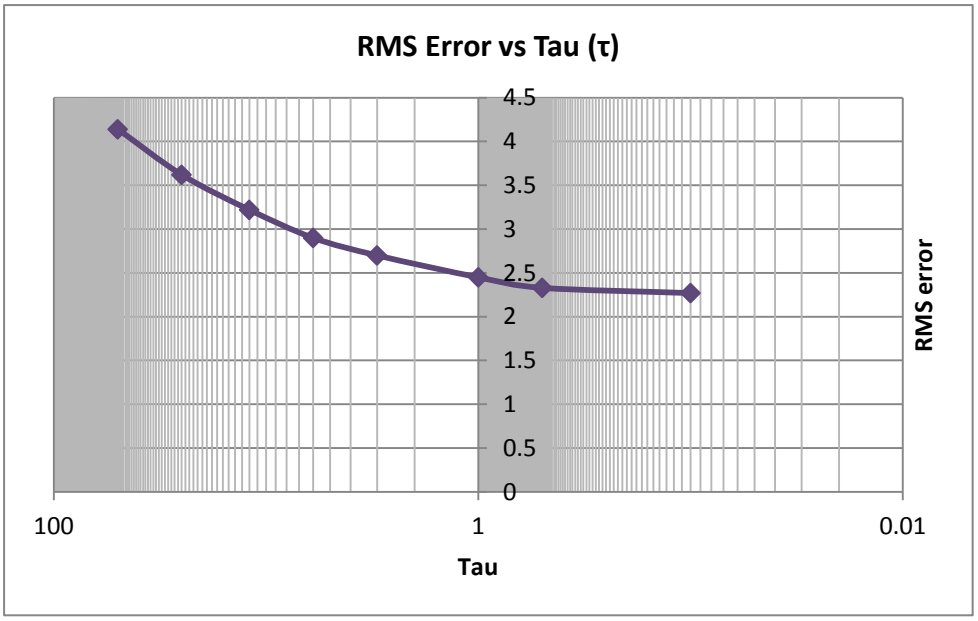

Figure 17, this graph is the 'trade-off' curve produced after the Tau (smoothing) factor tests. Tau three was chosen as it gives a low enough RMS error without losing meaning from the data as begins to happen when the curve tails out.

There are also two other smoothing factors which affect the model; alpha (α) and beta (β). To find the best fit for the data and the lowest RMS error these were thoroughly tested (Figure 18). Beta controls the relative smoothness of the deeper and shallower parts of the model whereas alpha controls the horizontal smoothness of the model. Beta is an exponential factor so will have a greater effect on the model than alpha which is a multiplicative factor. After multiple test inversions, it was decided that alpha of 1 and beta of 0.5 gave the best fit to the data. At this point all the tests had been done on the EMC profile - an identical mesh was created for SLA and the same optimal inversions parameters were used.

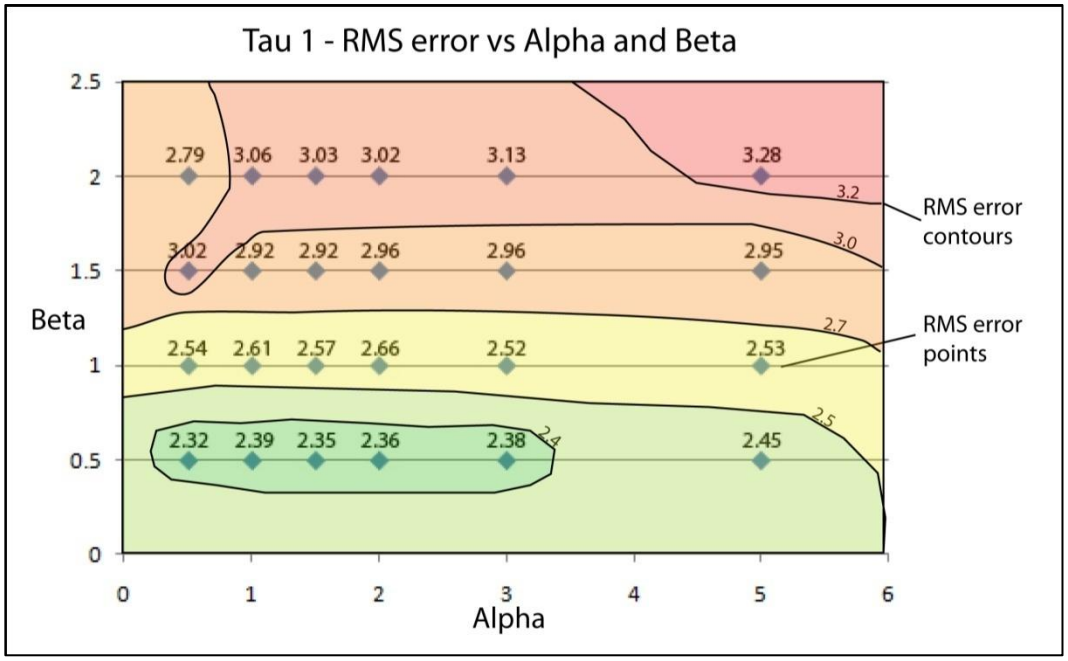

Figure 18, the image shown above gives the results for the alpha and beta factor testing at a Tau value of 1 for the EMC line. These tests were carried out for Tau values of 1, 3, 6 and 12 for completeness. The aim of these tests is to ensure the correct imaging factors which give the best fit to the data, i.e. the lowest RMS error hence only those within the green contour were considered.

When modelling, the aim is to converge on the lowest RMS error possible or the 'best fit' to the data. To achieve this objective, different weighting can be given to different data types; TM Phase, TE Phase, TM apparent resistivity, TE apparent resistivity and Tipper. The weighting is achieved by manipulating the error floor – a high error floor provides a low data weighting. The first inversion was set at 50% resistivity error floor and 5% phase error floor – the inversion process was started with a tighter control on the phase data rather than the resistivity data as the latter can be effected by static shift. The TE resistivity mode is also sensitive to 3D effects both in the subsurface and potentially in topography. Several different inversion orders or strategies were used (in all cases, TE and TM phase error floors were set at 5%):

1. Both TE and TM mode apparent resistivities (rho) set to 50%, then 25%, then 10% error floor. The Tipper data are then introduced with an absolute error floor of 0.1 (10% error).
2. Both TE and TM mode resistivities set to 50%, then 25%, then TE left at 25% and TM reduced to 10%. The Tipper was then introduced.

3. Tipper inverted first (error = 0.1) with TE and TM rho and phase both at 50%. The TE and TM phase 5% and rho 50%, then TM rho reduced to 25% and 10% with TE rho at 50%, and then TE rho reduced to 25%.

The third method was chosen to produce the final model as it gave the best resolution of the geological features, however the variations between the models do help identify which model features are robust and which are subject to the choice of inversion parameters. (See Appendix 2 for full images of inversions)

It was found on all profiles that when the TE mode apparent resistivity error floor was reduced below 25%, the RMS errors jumped up and the model became distorted, - an effect potentially due to the 3D topographical effects present within the actual data that cannot be captured in a 2D model. It is also be possible that there are 3D geological structures which the TE mode is more sensitive to.

Testing the robustness of the final model is needed to ensure the best possible fit of the model to the observed data and to what extent moderate perturbations to the final model can be accommodated and which features in the model are absolutely required and which features are not required (i.e. weakly constrained), so we can accurately represent the subsurface resistivity structure. The RMS error for the final model was recorded in an excel spreadsheet and each significant subsurface feature was then tested and the RMS errors recorded. Resistive features in the model were tested by firstly bringing up the base, by making the blocks below the resistor as conductive as the surrounding country rock, and seeing how far it was possible to reduce the basal depth until the RMS error was too high and the fit unacceptable (Figure 19). This method was then repeated, but to increase the thickness of the resistors. This approach was repeated for all significant features of both the EMC and SLA profiles (See Appendix 4 for full tests and results).

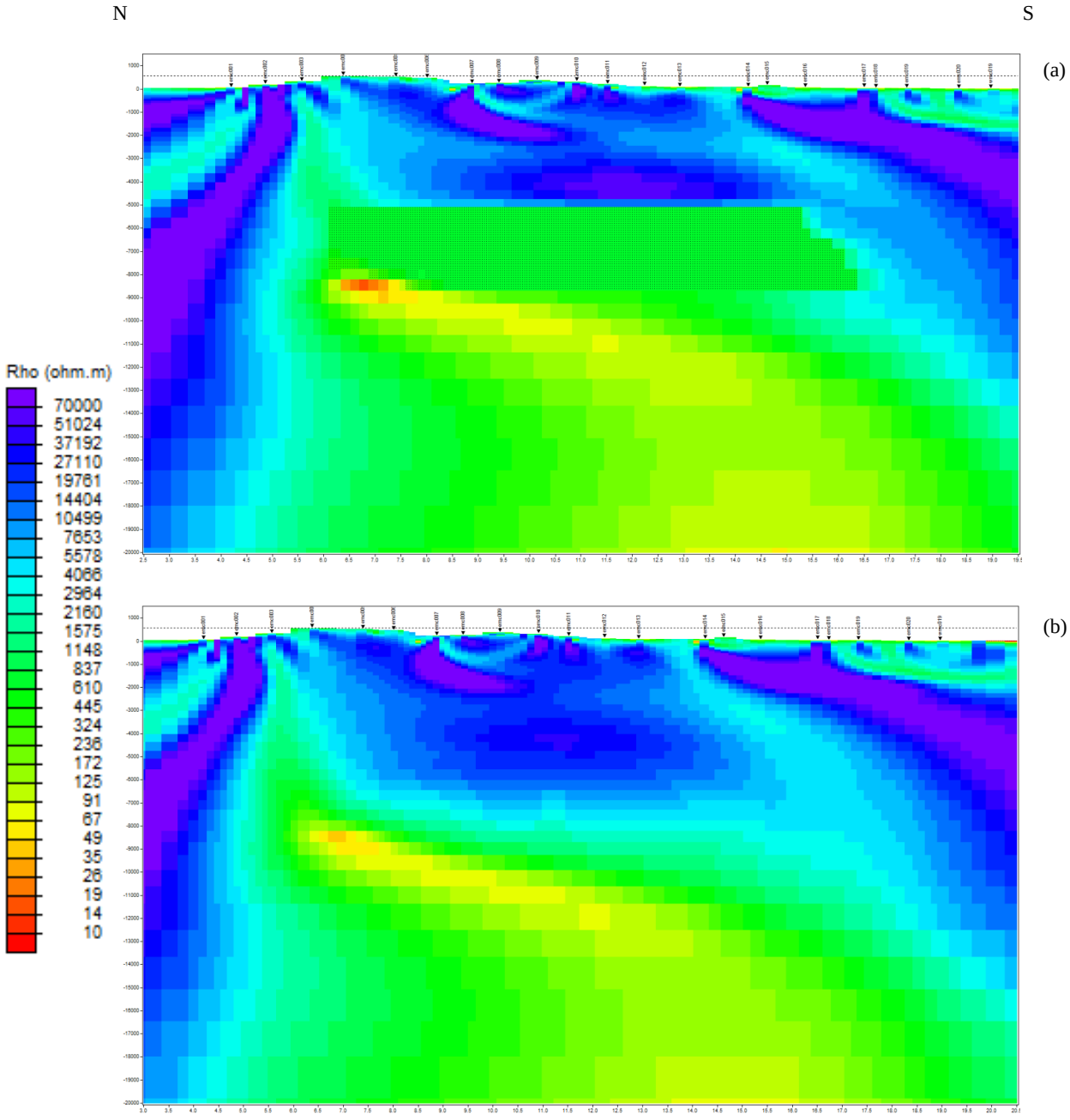

Figure 19, (a) is an example robustness test, (test 3 on the EMC line) where the central block on the EMC profile was reduced in depth. This model was then put through a full inversion where it one case (a) the teat area was locked so the program could not change it and (b) where the program was allowed to change the test area. Image (b) represents the norm for the tests as it reverts back to a similar shape and geometry to the original model.

4. RESULTS

4.1 The Eastern Profile – Line EMC

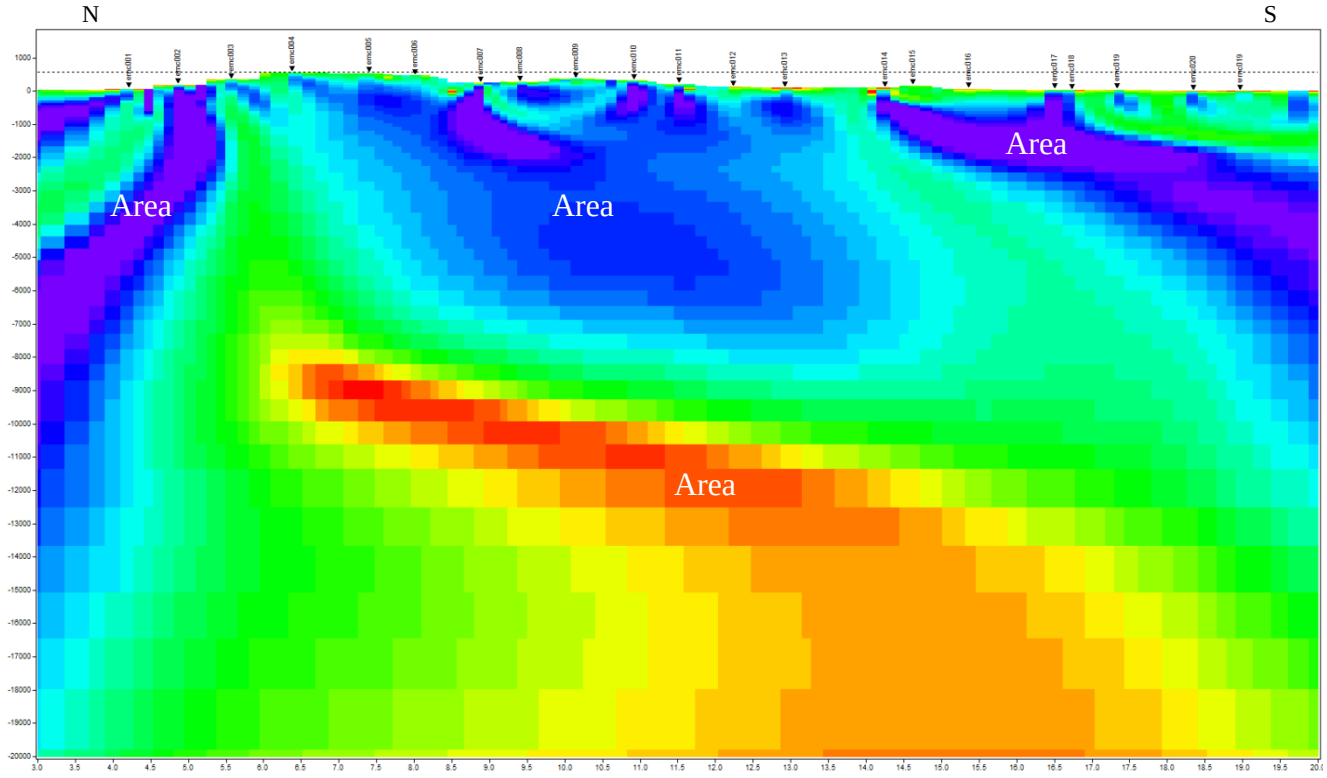

Figure 20, this is the final 2D MT model for the EMC profile line. The model extends down to 20km. Areas 1-3 are resistive and interpreted as granite, area 4 is a lower crustal conductor which is interpreted as a shale, clay or saturated lithology, scale below.

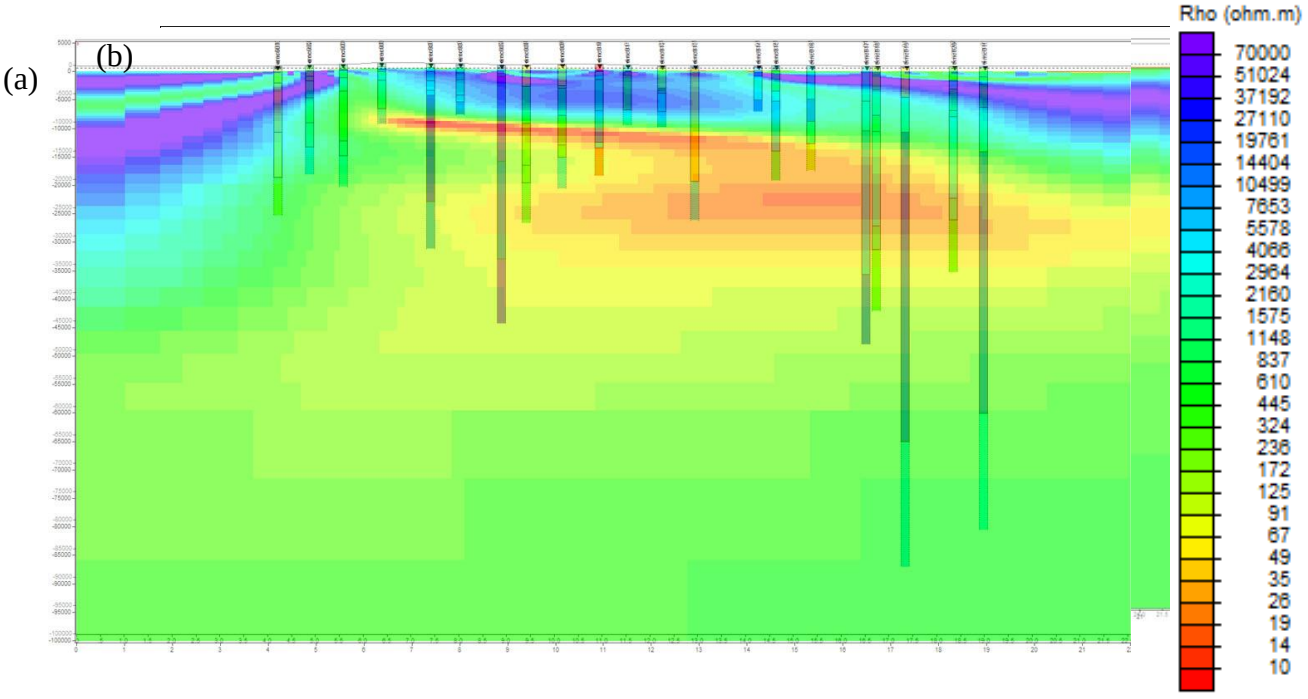

Figure 21, (a) shows the depths of penetration for the TE mode, the diagram extends down to 100km. The model should be ignored below the depths of maximum penetration. (b) Shows the depths of penetration for

each site for the TM mode, the diagram again extends to 100km and is unreliable below these maximum depths.

The image shown above (Figure 20) shows the final MT model produced for the eastern line. A preliminary assumption was made that any resistive areas around or above 10 000 Ohm.m were likely to represent granite and any surrounding, more conductive areas, were likely to be the shale country rocks. The Geological Survey of Northern Ireland have drilled a 600m deep borehole within the Silent Valley area of the Eastern Mournes pluton and from their down-hole resistivity measurements the granites range between 10 000 and 30 000 Ohm.m, and so, this was taken as an estimate for the resistivity of the granites within our profiles. Figure 21 gives a visual representation of the estimated depths of penetration at each site for both the TE and TM modes; the model is unreliable below these depths and should be ignored. However, it is worth noting that the width of penetration at any given site is approximately equal to their depth at that point (so a site reaching 10km depth would also be recording for 5km each side of it). Figure 20 shows what appears to be a moderately dipping granitic zone in the south below sites emc014 through to wmc019 at the end of the profile, a central granitic block extending from site emc003 to emc013 extending down to around 8km depth with a possible geological boundary through the middle and a northern granitic zone which is steeply dipping below site emc002. These granitic areas are surrounded by areas which are green in colour (approximately 400 Ohm.m) and are likely to be the shale country rocks. A large lower crustal conductor can also be seen at around 10km depth in the north, extending down to 30km in the south. This model has been robustly tested to ensure it gives the best fit to the data, part of this included shallowing and deepening all of the above mentioned resistive areas. The fit to the data got considerably worse when any of the areas were decreased in depth by even a small amount which would suggest that this model shows the minimum depth for those resistors, however they were more accommodating to increases in depth, although only by a few km. Nevertheless when put through a full inversion run both the shallower and deeper models reverted back to a similar depth as in the original model suggesting this is the most likely fit. The conductive areas between the granites were also tested to see if it was possible that the granite extended through these areas, however when these areas were modelled as resistive blocks the fit to the data was much more erroneous and so if these blocks are connected it must be out of the plane of this profile and would require a 3D model. For full testing results see Appendix 4.

4.2 Interpretation and discussion of profile EMC

The northern resistor (Area 1)

The region named as area 1 in figure 20 shows the steeply dipping resistor mentioned before; this feature is quite unusual and was unexpected, the laccolithic model predicts no vertical resistors at the northern end of the profile, indeed, no resistors extending below around 3km depth. It could be explained more easily using the cauldron subsidence model, however, that would require a feeder chamber or zone below the feature as it is unlikely the more buoyant magma would have travelled downwards for any considerable distance, therefore this feature was heavily tested (Tests 1,2,7,9 and 10 EMC in Appendix 4). Unfortunately site emc002 was plagued with noisy data and so during the editing process a large portion of data was removed (Figure 22) from 10^{-2} through to 10^{0} seconds in the TM mode, which would relate to the depth range around 1500m to 50km. The TE mode at this site has a much smaller depth of penetration and reaches around 20km (Figure 21) so when taking this into account the model becomes unreliable between 20 and 50km below site 2. The TE mode seems to require a lower crustal conductor as seen at the adjacent sites in the profile, however when such a conductor was introduced into the model (Test 9, Appendix 4) it was not accepted by the data. This is likely due to the parameters used when modelling, as mentioned in Section 3.4 a tighter constraint was placed on the TM data over the TE data due to the potential topographical effects contained in the TE mode which could not be modelled and this may have forced site emc002 to try and fit to the poorly constrained TM data rather than the better TE data. The next site with considerable depths of penetration is be site emc005 which may provide more of a constraint on the characteristics below site emc002, site emc005 also requires a lower crustal conductor at around 20-30km, with an increase in resistivity below this, at around 50km depth which likely corresponds to the mantle. Therefore it can be concluded that down to around 1.5km the model is tightly constrained and that this vertical resistor must be accounted for in the emplacement model, down to around 20km the model is fairly constrained but between 20 and 50km it is not constrained by emc002's data and is more likely to be conductive than resistive from the adjacent data. It may also be worth noting that site emc002 is located on or very closely to the boundary between the granites and the country rock at the surface (Figure 7), this gives the site is a strongly 2D geometry which may have some effect on the model.

(a)

(b)

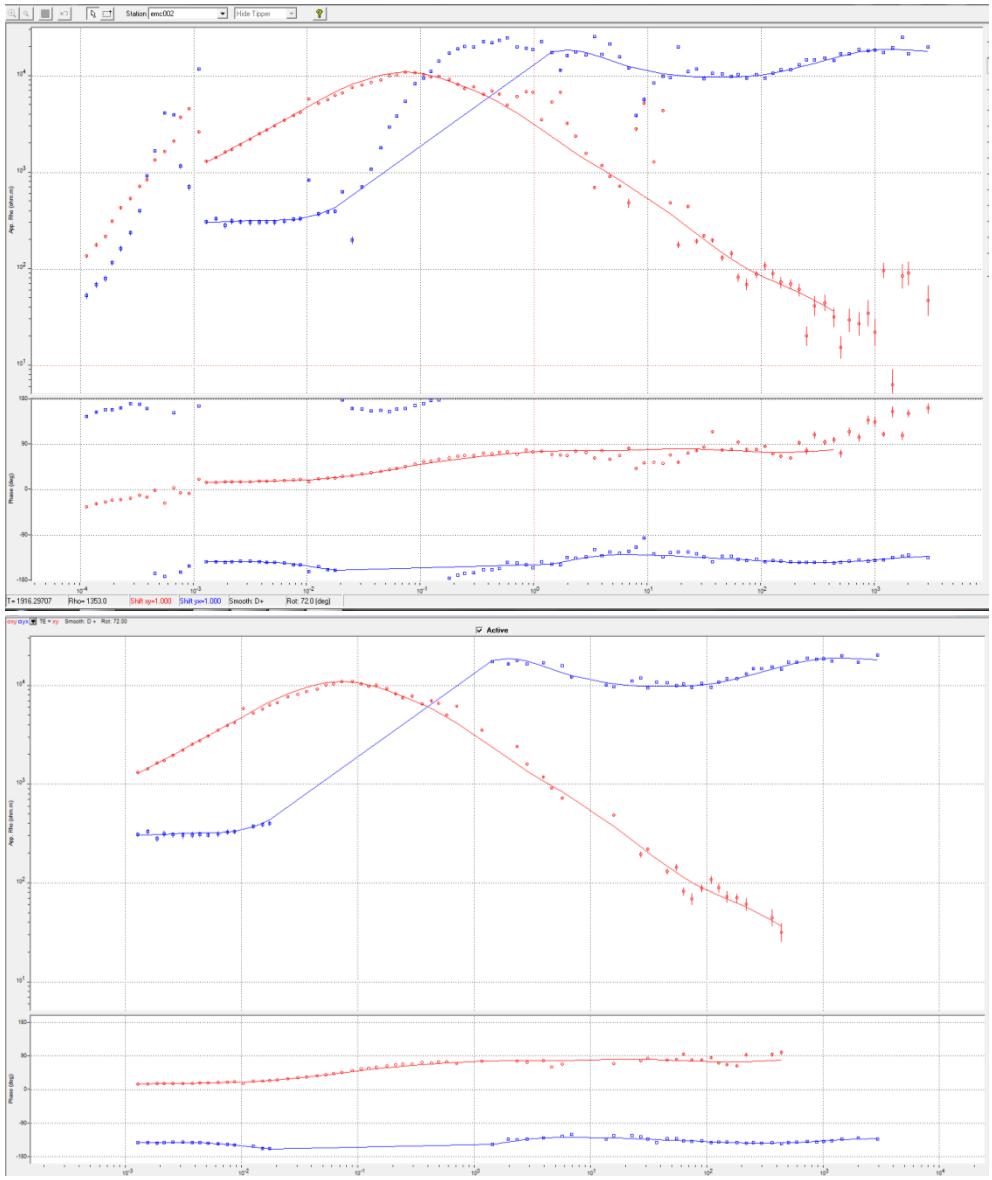

Figure 22, (a) and (b) show the MT data for site emc002. (a) is the unedited data and (b) the edited data. This site was one of the noisiest within all of the profiles and the data was not D+ consistent so a large portion had to be removed which, unfortunately, in the TM (blue) mode related to depths ranging from 1500m to 50km.

The central resistor (Area 2)

Area 2 in figure 20 shows the central resistive block which is located roughly under the outcrop of the Eastern Mournes pluton; the outcrop at surface extends from site emc002 to site emc012. You would expect therefore that the model at the surface between these sites would be very resistive probably around 10 000 Ohm.m or more, however as can be seen in figure 20 the upper few hundred metres is fairly conductive and looks more like the country rocks, this can be attributed to the weathering of the granites. The

weathering process will break the granites down making them more conductive, an example of this would be the degradation of the feldspars to clay which is much more conductive. In a near-surface geotechnical study, Olona *et al.* (2010) measured the resistivities of fresh through to weathered granite in the Carlés granite in North-West Spain and found that when weathered the resistivity was reduced from around 3000 Ohm.m to just 60 Ohm.m. It is also likely that the weathered granites are more porous so they will contain a higher amount of groundwater making them again more conductive. The feature seen between sites 7 and 10 could be a deeper extent of this weathering where the water has taken advantage of a weaker zone – possibly faulted- and percolated downwards. It is also worth noting, that the thickness of this top layer is not as well constrained as the rest of the model, due to noisy data at higher frequencies which has been edited out. Interestingly the central block is deeper than predicted by the laccolithic model (~3km) and yet shallower than predicted by the cauldron subsidence model (~10km), at first glance it has the shape predicted by the cauldron subsidence model, however it lacks the magma chamber or feeder below which would have caused the block of country rock to sink (Anderson 1936). When looked at in more detail, the central block has a more resistive top 3km with values around 120 000 Ohm.m and the bottom 5km around 30 000 Ohm.m, it can also be seen that on both the northern and southern sides of the central block the resistivity contours appear to pinch in at around 3.5km suggesting that there is a slight separation of the two areas. It is likely that this represents a geological boundary with a more fractionated granite above and a more basic below, the reason it is not more distinct on the model is because the lithologies are too similar in resistivity. It is known that at the surface three granites outcrop with major and minor variants within these (Hood 1981) however none of these differences can readily be seen on the model as the granite lithologies have resistivities to similar to each other to be recorded by the MT method. When you take this into account it is very possible that this lower area does represent separate granite and so we have two thin sheets around 3km in thickness rather than one large 8km intrusion.

The Southern resistor (Area 3)

Area 3 displayed on figure 20 shows a southerly dipping resistor which clearly shows that the granites do extend to the south of the area, agreeing with the positive Bouguer gravity anomalies, (Reay 2004), which suggested that the granites would extend to the south toward a large gravity anomaly just offshore which is believed to be the magma chamber/source. The AMS data from Stevenson *et al.* (2007) also predicted a southern

extension of the granites from a linear fabric of the granites extending SSW/NNE which was thought to represent the magma flow direction. The model seems to agree with these findings suggesting that the magma flowed upwards from the south and then flowed laterally across. The smaller resistive areas above the main body could represent slices through offshoot dykes or sills from the main body; these have been well documented in many intrusions (Petford *et al.* 2000; Vigneresse 2004; Horsman *et al.* 2010 and Bunger & Cruden 2011 among many others). Interestingly site emc015 lies on top of the Glasdrumman dyke which is Quartz-feldspar and feldspar-porphyry in composition, however there is no evidence for this on the model, underneath emc015 it appears as a similar resistivity to the country rocks. This is a significant finding as it was always believed that this dyke which partially surrounds the eastern pluton was a ring dyke representing the magma conduit for the cauldron subsidence model. Of course the depth of penetration needs to be considered for this site and it is between 200 and 10 000m; this suggests that the dyke must be less than 200m in depth extent.

The lower crustal conductor (Area 4)

The area marked as number 4 on Figure 20 is a conductive region in the model varying from 1 or 2 Ohm.m to around 60 Ohm.m, if you refer back to the electrical properties table (Figure 6) you will see that these figures could relate to graphite, weathered ultramafic rocks, clays, shales, lignite/coal or water (saline-fresh). The suggestion that this conductor could also be due to sulphide mineralisation was considered, however, it was concluded that the area should be less than 1 Ohm.m if this was the case. Ultramafic rocks can probably be ruled out as it has been shown by McCormick *et al.* (1993) and Meighan (1988) that the Mourne granites are not derived from a purely mantle source and even an enriched basalt could not produce the values $\delta^{18}O$ and $^{87}Sr/^{86}Sr$ values seen, therefore it is unlikely that a large ultramafic intrusion would be located in this area and almost impossible that it would also be weathered. Lignite/coal/graphite is also extremely unlikely; if we assume a continuation of the Silurian sediments down to this depth then at the time of their formation the conditions at the surface were not likely to be suitable for such a large organic deposit. The greywacke country rocks were deposited in a deep marine environment during the early Silurian (Llandovery) in the Iapetus ocean. This was a very tectonically active time; the Iapetus Ocean was rapidly closing as it was subducted underneath Laurentia. This seems an unlikely setting for any organic deposits, they are more likely to be destroyed in this environment if such a large deposit could even have occurred (Anderson 2004).

Therefore we are left with water, clay or shales and each of these seems like a reasonable explanation. The Mournes are located on a large jut of land which has the Irish Sea on one side and the Carlingford Loch on the other; therefore it is not impossible to assume that a porous and permeable lithology at depth could contain significant amounts of water which must be slightly saline to produce such a conductive area on the model. It is also not impossible to imagine an older shale or clay lithology lying underneath the Mournes in this area. Robbie (1955) reported that the granites of the Eastern Pluton are considerably altered to clays including kaolinite and montmorillonite and that this occurred during a hydrothermal phase, of course it is much less likely that this conductor is an area of severely altered granite rather than a separate lithology but it is not impossible. Although as mentioned before electrical conductivity does not just depend on the electrical properties of the rock minerals. Temperature, pressure, porosity, permeability and the physical and chemical states of the rocks can also play a part.

4.3 The Western Profile – Line WMC

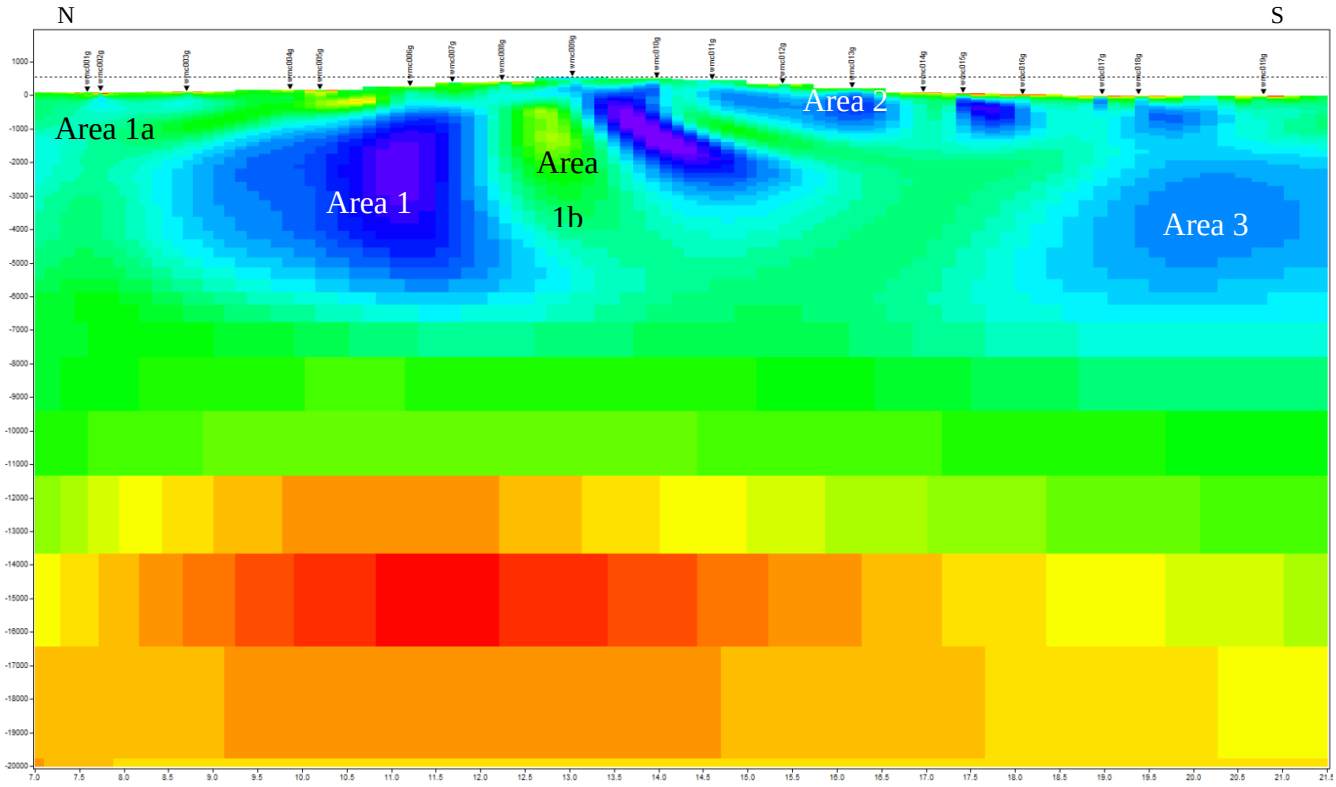

Figure 23, this is the final 2D MT model for the WMC profile. It extends down to 20 km. Areas 1-3 are resistive and interpreted as granite. Area 4 is a lower crustal conductor and interpreted as a clay, shale or saturated lithology. The model is taken from Yeomans (2011). Scale for resistivities next to figure 25.

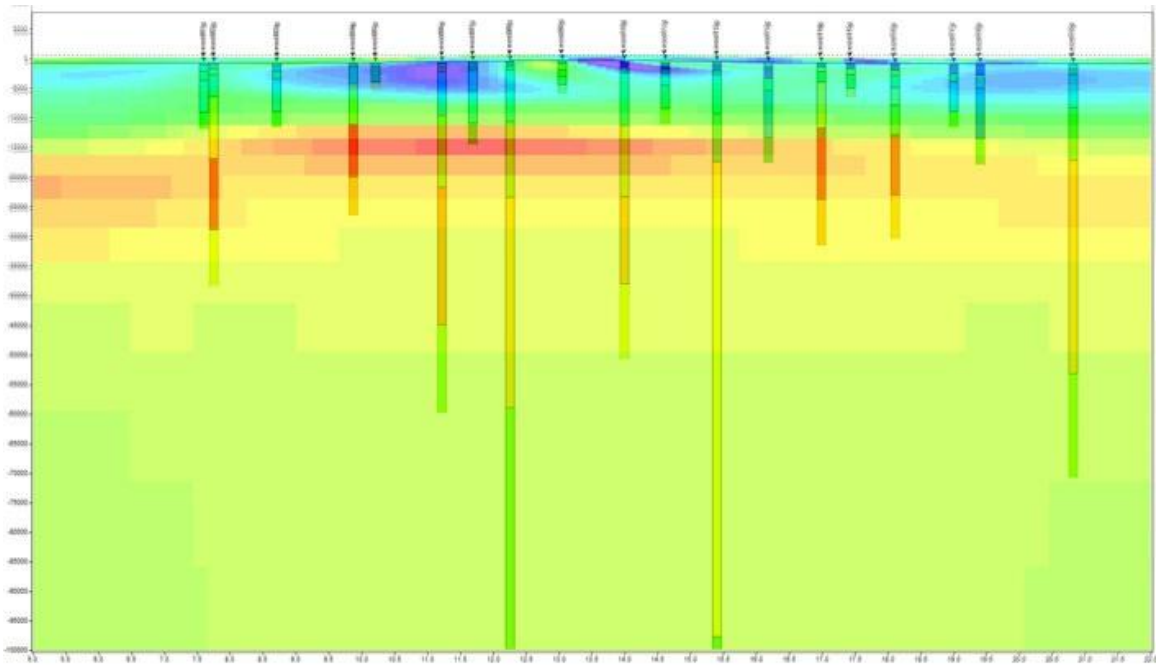

Figure 24, this image shows the depth penetration of each sites data for the WMC profile. This model also extends down to 100km. This model shows the invariant (or the average) of the TE and TM modes of penetration. The model is unreliable below this depth and should be ignored. Model taken from Yeomans (2011). Scale for resistivities next to figure 25.

Figure 23 shows the final MT model for the Western Mournes pluton, the resistive areas (blue/purple) were again at least 10 000 Ohm.m and so using the Silent Valley Borehole data were taken to be granitic. Figure 24 shows the depths of penetration for each site for the WMC profile line, the model is unreliable below this and should be ignored. The model shows again a large central resistor underneath the mountains, however not as deep as on the eastern side; only reaching around 6km. It also has a large conductive area in the centre of it beneath sites wmc008 and wmc009 which also reaches around 6km. There is a granitic body inferred to be a feeder zone in the south of the profile similar to that seen in the eastern profile underneath site wmc019 which extends to around 7km depth and appears to be at least 4km in thickness; however it must be remembered when looking at this western profile that the orientation of it is slightly oblique to the predicted SSW/NNE magma flow direction by Stevenson & Bennett (2011). The station wmc019 is also present on the eastern profile line (figure 20) which is parallel to the predicted magma flow direction from Stevenson *et al.* (2007). This suggests that the area imaged underneath wmc019 may in fact be a slice through the

eastern feeder zone and that the thin granites between stations wmc011 and wmc016 may represent an oblique slice through a thin, tabular feeder zone for the western area as imaged in the southern profile (figure 27). The model was again robustly tested (Appendix 5) including the depth of the granites; similarly to the eastern line, the data would only accept a small reduction in depth (~1km) but would accept a larger increase in depth (~2/3km), but still reverted to the original model when put through a full inversion run again. This suggests that the modelled depths are a minimum depth but also the best fit to the data. The large conductor (Area 1b) was also tested (Test 4 Appendix 5) and it seems that it is required by the data.

4.4 Interpretation and discussion of profile WMC

The central resistor (Area 1)

Area 1 shown on Figure 23 is a large granitic body extending down to around 6km depth underneath the Western Mournes pluton, the outcrop of granite at surface level is half way between sites wmc004 and wmc005 and between sites wmc012 and wmc013. Similarly to the eastern profile the top few hundred metres below these sites are more conductive than would be expected but it can be attributed to the weathering of the granites as discussed in section 4.2. This central resistor extends deeper than predicted by the laccolithic model (~3km) and is not tabular in shape, however it is much shallower than predicted by the cauldron subsidence model (~10km) and there is no evidence for any magma source directly below the pluton either. Therefore it is more likely to have been intruded as sheet which has inflated more than expected. Area 1b highlights the large conductor in the middle of this central resistor; the data require this conductor to be there as during testing (Test 4 appendix???) it was replaced with resistive material and put through a full inversion and a full inversion where the new resistor was locked (Figure 25).

N S

(a)

(b)

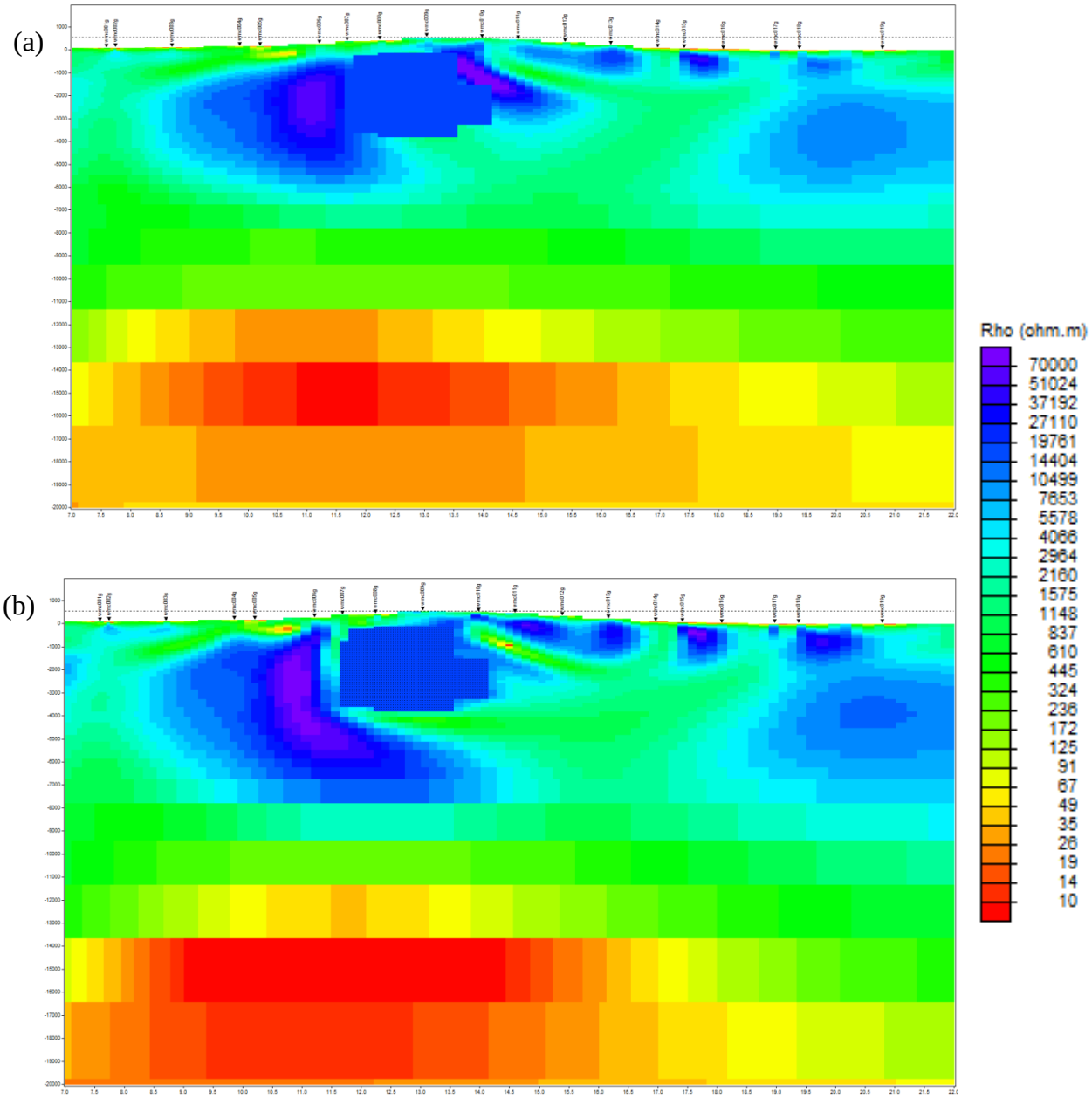
Rho (ohm.m)
70000
51024
37192
27110
19761
14404
10499
7653
5578
4066
2964
2160
1575
1148
837
610
445
324
236
172
125
91
67
49
35
26
19
14
10

N S

(c)

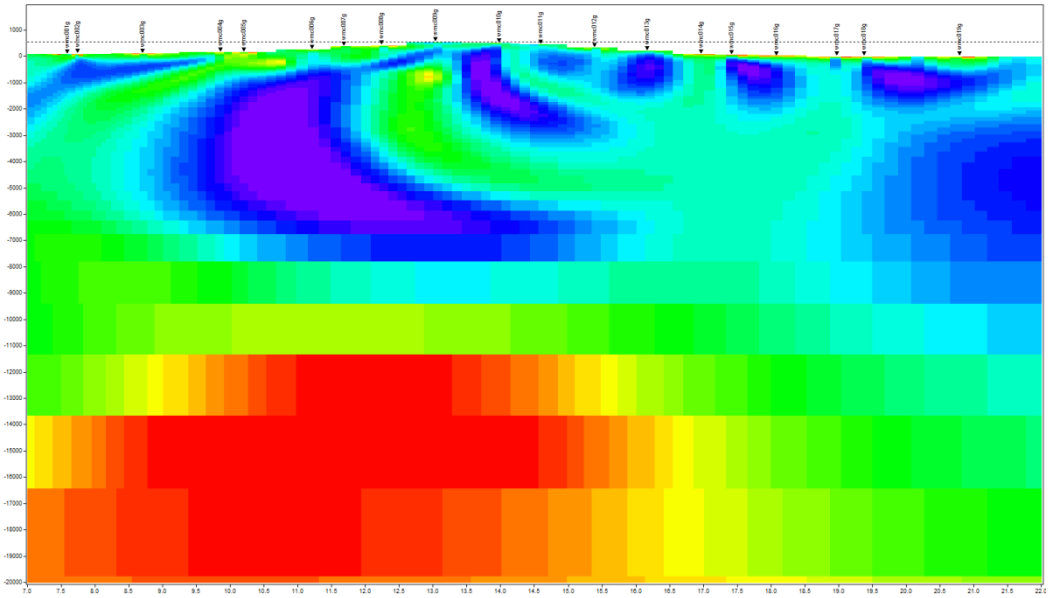

Figure 25, these three images show test 4 of the WMC robustness tests. Test 4 was completed to check if the model would accept a continuation of the granite. (a) Shows how the granites were connected with resistive material. (b) The results of the locked inversion and (c) the results of the unlocked inversion. It can be seen on image (b) that the inversion process has re-entered the conductor at the left hand side of the new resistor, this suggests that the data absolutely require the conductor to be present within the model. These tests have also changed other parts of the model including the lower crustal conductor, this has been made larger and more conductive to try and offset the shallower changes. Model and tests from Yeomans (2011).

In the unlocked inversion, the model reverted back and replaced the original conductor (Figure 25 c) and in the locked inversion it has placed a small conductor at the edge of the locked area (figure 25 b) suggesting that it is a required element. Interestingly the RMS errors were not significantly higher for the latter model (Test 4c, Appendix 5) suggesting that the thickness of this conductor in the final model possibly represents a maximum width. This conductive zone has a similar resistivity value to the surrounding country rocks, however it seems unlikely that a raft of country rock that size would have been broken off by the magma and remained un-metamorphosed to appear as conductive as the more distant country rocks. As a rock becomes more metamorphosed you would expect it to also rise in resistivity value (Figure 6). It is possible that the conductor could represent a fault zone within the granite body; if this fault zone had fluids within it, especially if they were rich in conductive elements, then it would show up as a conductive zone. There is a large fault within the western pluton which outcrops at the surface, yet it is located at site wmc005 and the conductive area at depth is below sites wmc008 and wmc009. This then seems unlikely to be a deeper continuation of the fault mapped at the surface, yet the presence of this large fault at surface does make it more likely for another large one to be present at depth. Sites wmc001 and wmc002 are

sited on the Newry Granodiorites which are located to the north of the Mournes and are more mafic in composition, especially at their edges (Cooper & Johnston 2004). This area, indicated by 1a on Figure 23 is characterised by resistivities between 3000 and 5000 Ohm.m and so is less resistive than the Mourne granites, yet more conductive than the country rocks, so is believed to be the edge of the Newry intrusion.

The two southern resistors (Areas 2 and 3)

The area marked as area 2 on figure 23 consists of a series of small granitic "spots" between sites wmc011 and wmc016. These isolated resistors have been tested to see whether the data would accept a continuation of the granite, rather than separate areas, but the fit to the data was not acceptable. This suggests that either any potential connections must be out of the plane of this profile, that the feeder zone was composed of a series of propagating sills or that it was in fact a single sheet that has later been faulted. Section 4.6 discusses the southern line cross section through the same sheet which is also separated into distinct areas; from the testing of the southern line (Test 1 SLA, Appendix 4) there is evidence for the isolated resistors to be separated by faults. This would make it more likely that those imaged by the western profile were also separated by faults, but during the testing of the western profile the features were adverse to being connected and would revert back to a separated configuration (Test 3, Appendix 5) - Unlike those on the southern line which accepted being connected by both conductive and resistive material. The fact that the western profile is oblique to the proposed magma flow direction from Stevenson & Bennett (2011) means that we may be looking at more of a cross section through the western feeder rather than along it, these isolated granites could therefore be explained by the feeder zone being composed of a series of propagating sills which in some cases were never connected, or they were not completely connected. This mechanism has been documented in large sills where there is evidence of smaller pre-cursor sills by Hutton (2009).

Area 3 on figure 23 shows a large granite body below site wmc019, which is more likely to be the larger EMC feeder. The eastern line, unlike the western, is located parallel to Stevenson *et al's* (2007) NNE/SSW magma flow direction and so we would expect to see all aspects of the complex. However, with the western profile being oblique to flow, the feeder for this pluton is likely to be located to the west of the profile line (Figure 26). This large granitic body cannot conceivably be feeding the western body as well as the eastern body, as Stevenson & Bennett's (2011) proposed magma flow direction for the western centre from their AMS data was also NNE/SSW and from site wmc019 this direction points toward the eastern centre.

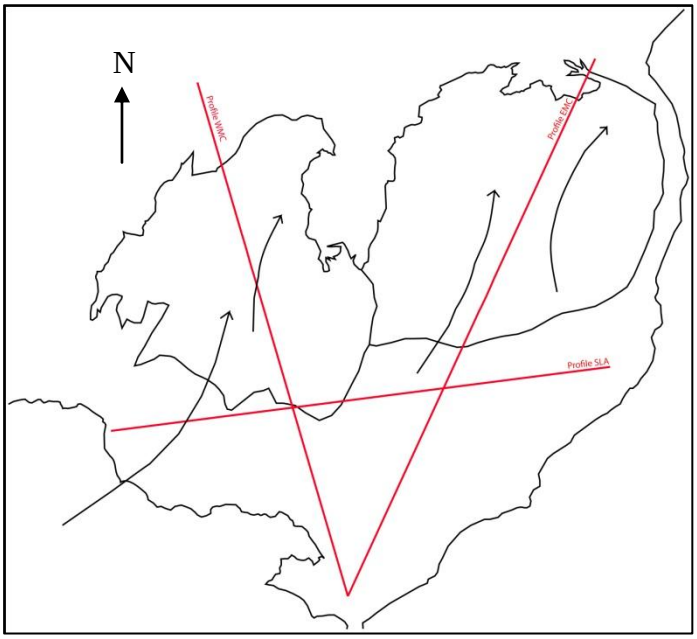

Figure 26, this schematic diagram shows the proposed direction of magma flow after Stevenson *et al.* (2007) and Stevenson & Bennet (2011) in relation to the profile locations. As is demonstrated above, the eastern profile is parallel to the proposed flow and the western is oblique to it, giving a potential diagonal slice through the complex.

The lower crustal conductor (Area 4)

Area 4 shown on figure 23 is extremely similar to the lower crustal conductor on the eastern profile (Figure 20); it is a similar depth and size with almost the same resistivity values although it is less well imaged due to the coarser mesh at this depth. It is likely therefore that the conclusions drawn for the eastern profile in section 4.2 also apply here and that the conductive area/material extends underneath both plutons. Both explanations of the eastern profile conductor would fit with this observation; an older clay or shale lithology could easily extend under the western pluton as could a saturated

lithology; therefore although this observation gives more constraint on the size of the conductor it does not constrain further its origin. It may be significant that this conductor only appears directly underneath the central Mourne Mountains area, yet, it is hard to draw conclusions about the significance from these models alone.

4.5 The Southern Profile – Line SLA

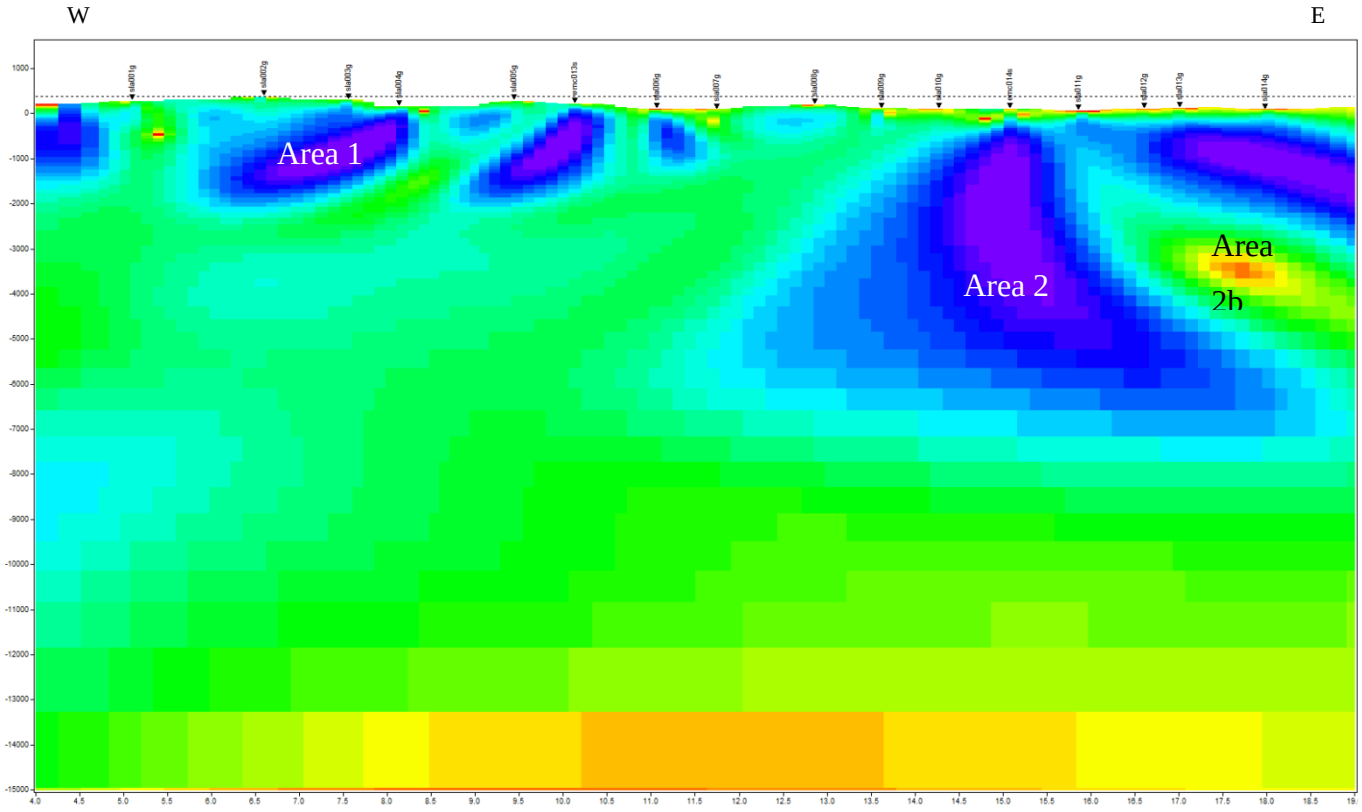

Figure 27, this is the final 2D MT model for the southern line. This model extends down to 15km. Both areas 1 and 2 are resistive and interpreted as granite, with area 2 extending deeper than area 1. Area 1 is interpreted as relating to the western pluton and area 2 as relating to the eastern pluton. See Figure 29 for resistivity scale.

(a)

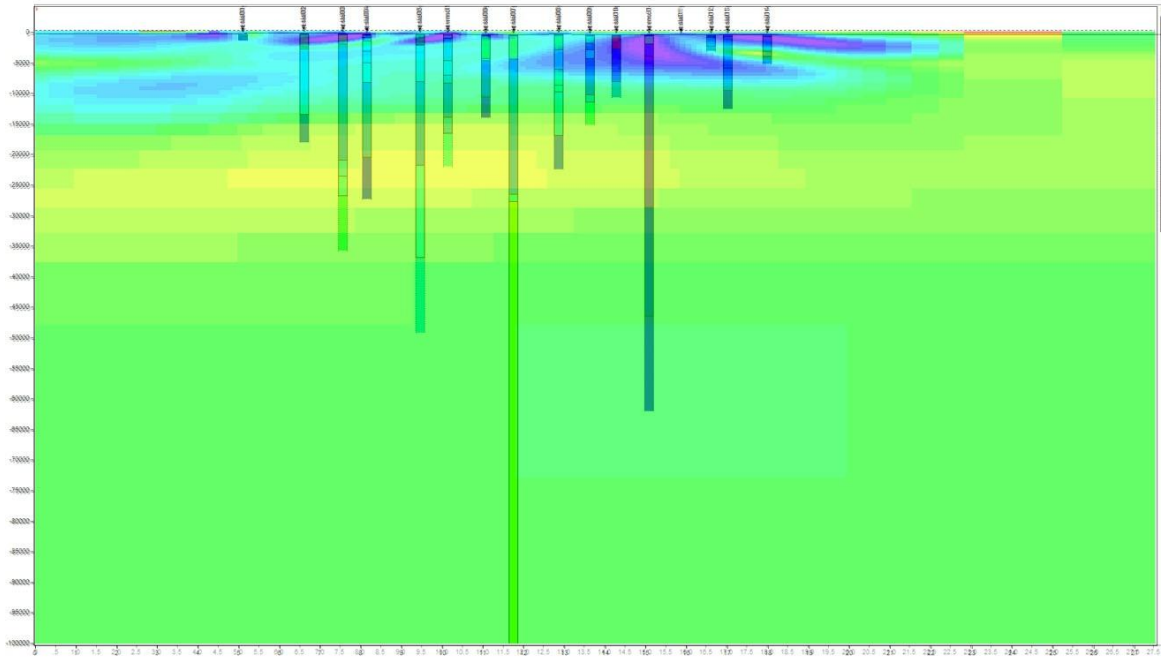

(b)

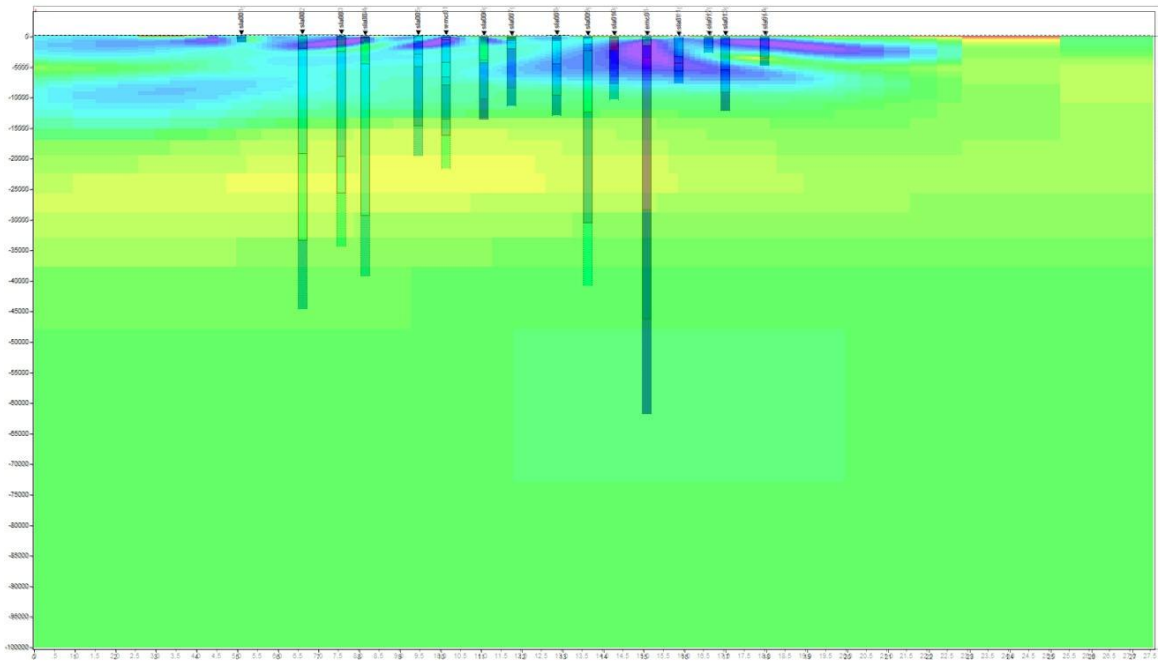

Figure 28, image (a) shows the depths of penetration for each site for the TE mode for the SLA line, and (b) the depths of penetration for each site for the TM mode. The model extends down to 100km and it is unreliable below these individual depths of penetration and should be ignored. See Figure 29 for resistivity scale.

Figure 27 shows the final MT model produced for the Southern profile. There are large resistive areas for almost the full width of the profile, but not reaching the surface. The left hand side of the profile relates to the western pluton and the resistive area here is much thinner than that of the right hand side which relates to the eastern pluton. Figure 28 shows the approximate depths of penetration for both the TE and TM modes of the SLA line data, the model is unreliable beneath these points. Using the Silent Valley borehole data we can again assume a baseline for the granites at 10 000 to 30 000 Ohm.m, which correlates to the dark blue/purple areas which we therefore take to be granitic. We therefore infer several thin granitic zones underneath the western side, not extending to more than 2km depth, between sites sla001 to sla007. On the eastern side we observe a large vertical granitic area underneath sites sla009 to sla011, but centred on site emc014 (this site is also the intersection with the eastern line) down to around 8km depth, with an easterly dipping granite body beneath sites sla011 through to sla014 extending from 1km to around 4km depth. The SLA model has again been robustly tested, including a shallowing and deepening of the resistive areas, which again were much more sensitive to a shallowing of the model and only allowed around a 500m

depth decrease before becoming extremely erroneous, whereas the depth could be increased by a few km with an acceptable fit. However, when the full inversions were run again the depth reverted back to the original, suggesting that this model represents the best fit but the granites could extend slightly deeper. The most interesting result for this profile is Test 1 (Figure 29) where the individual granite areas for the western side were connected with 10 000Ohm.m blocks and run through one full inversion and one full inversion where the blocks were fixed in place. In both cases, the RMS error was not significantly increased and during the 'unlocked' full inversion the model retained some of the higher resistivities between the blocks, unlike in the tests in the other areas of the model, where it reverted back close to the original model (Figure 27). See Appendix 4 for full test results.

(a)

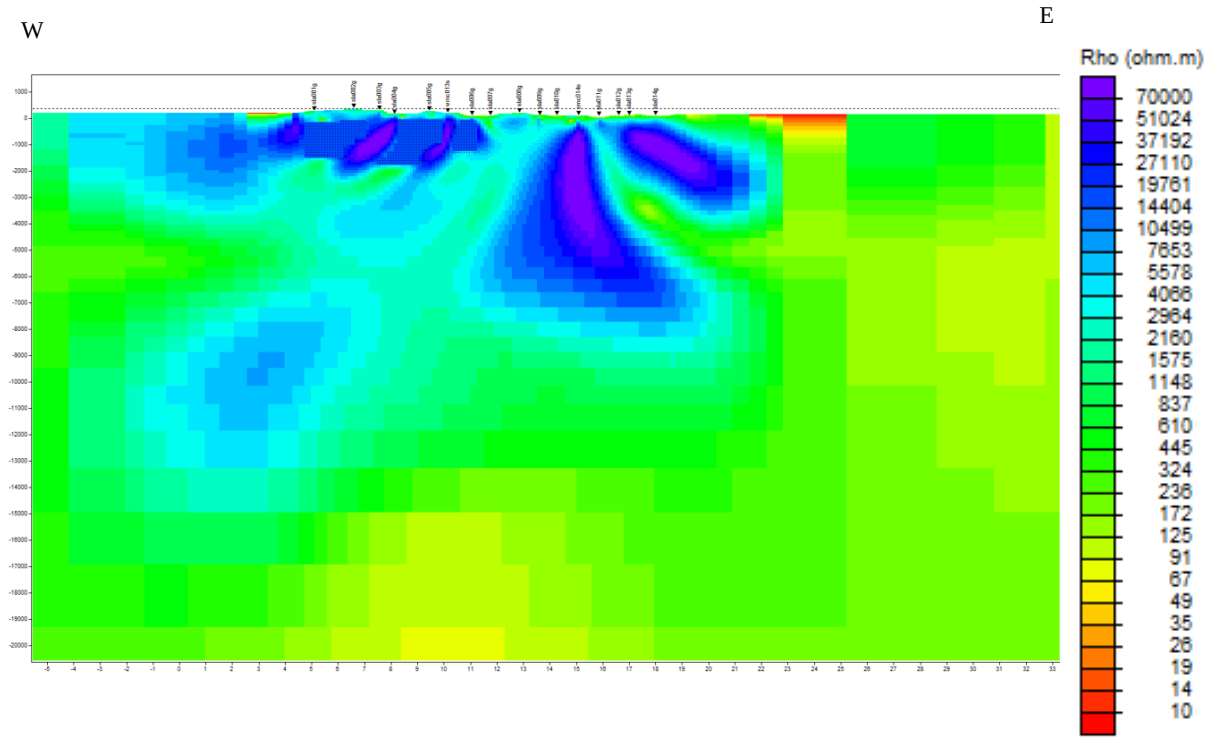

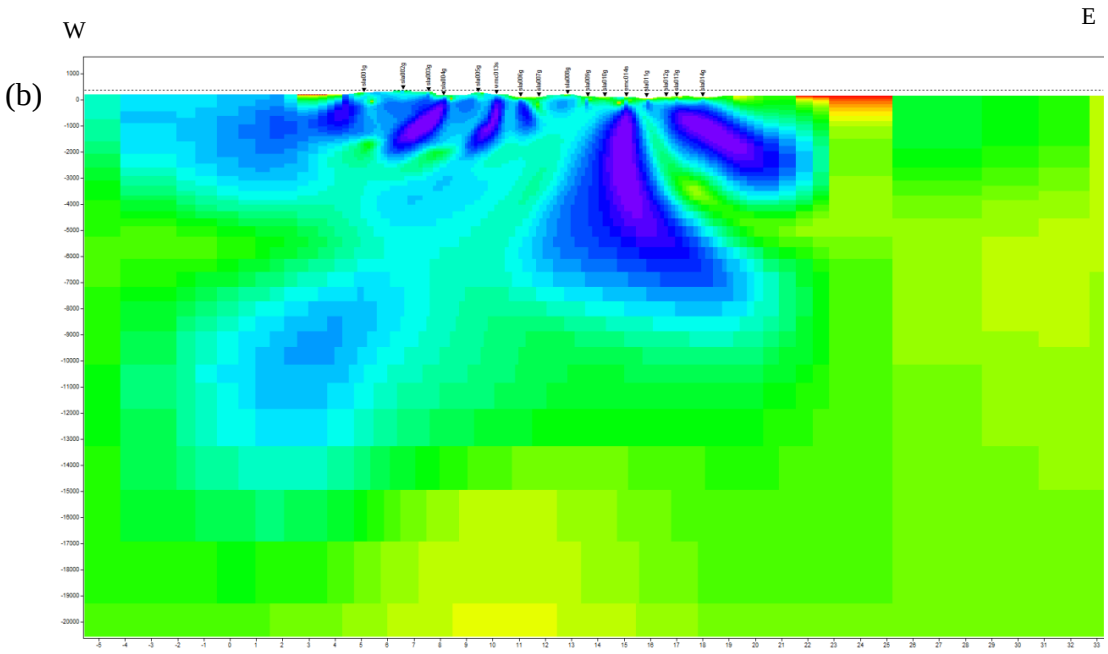

Figure 29, these two images show the robustness test 1 for the SLA profile. (a) Shows how the isolated granitic areas were connected with resistive material to test their connectivity. (b) Shows how the model has kept some of this resistive data rather than replacing the more conductive material. These areas where then interpreted as faults.

4.6 Interpretation and discussion of profile SLA

The Western resistor (Area 1)

The MT data imaging the western resistor, shown as area 1 on figure 27, seem to accept being connected by resistive or conductive material; this may be an indicator of a fault. If this is the case, we would have a thin tabular sheet of granite which has been faulted in several places either during emplacement or subsequently. This thin tabular sheet, which extends to the south on the WMC profile, was predicted for the Western Mournes by Stevenson & Bennett (2011) and this model confirms its presence. It is likely that the sheet does extend further to the south toward the positive Bouguer gravity anomaly, Figure 5, which would represent the magma source or feeder zone (Reay 2004). Interestingly this western sheet appears to overlie the eastern granite with a conductive area in-between them; this area has also been tested (Test 7) and the data does require it to be conductive. This area is likely to be a raft of country rock which represents the remains of the country rock which originally lay between the two feeder zones for the plutons. It is likely that these country rocks were rotated, bent and finally broken as the sheets expanded laterally and vertically during emplacement, finally causing the western sheet to overlie the eastern. This process has been documented at many scales

in basic and doleritic sills by Hutton (2009) and would suggest that the two feeder zones may merge together in other locations.

The Eastern resistor (Area 2)

The large vertical granitic body shown as area 2 on Figure 27 is located at the intersection between the eastern and southern lines. When you compare the two profiles it is apparent that emc014 (as shown on the southern line) is imaging the edge of the central resistor from the eastern profile (shown in figure 20 as area 2); from the southern profile then we can see that this central block is around 6km thick from W-E at the most southern edge. The shallow-dipping granite to the right of this area is very similar in size and orientation to the southern resistor on the eastern profile (area 3 on Figure 20), the suggestion that the two profiles may be imaging the same feature seems the most likely explanation, but would require the feeder zone to extend laterally to the east (figure 30).

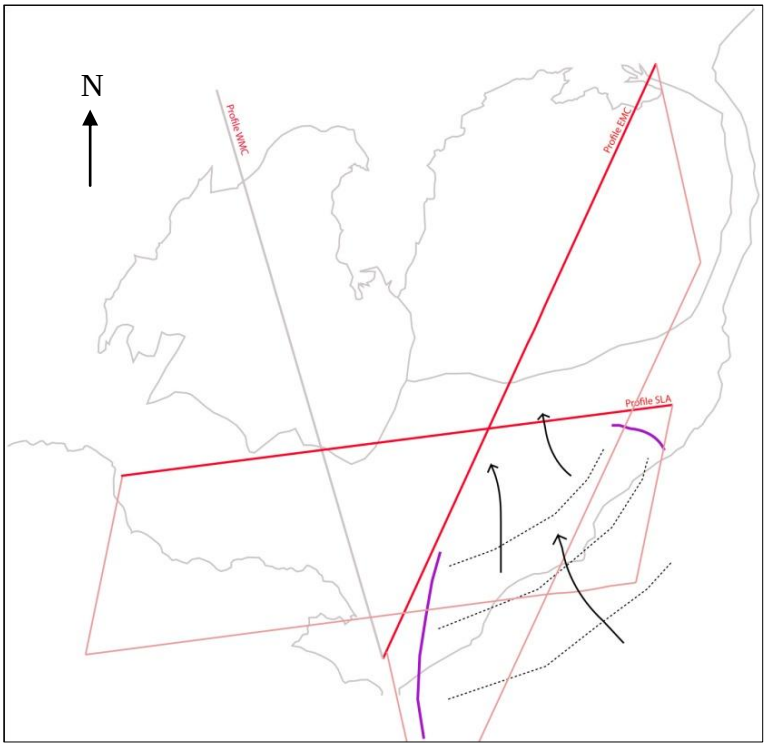

Figure 30, this schematic diagram show the end resistors of both the EMC and SLA profiles in a pseudo 3D interpretation. The geometry of these two bodies is remarkably similar yet if they were connected as shown above the magma flow direction would contradict the AMS data and the gravity data. However, it is a feature which should be further explored.

This explanation does seem the most likely, however when you consider the predicted magma flow direction of NNE/SSW from Stevenson *et al.* (2007), the data don't seem

to agree. There is also no Bouguer anomaly located onshore or offshore in this area. It is possible that it could represent an offshoot dyke or sill as it does not extend to great depths, reaching only around 2km, although it does appear to be deepening at the eastern cut-off of the model. It also doesn't connect to the main body of granite; however neither does the feeder on the eastern profile. Extra MT sites on the southern line are really needed to determine the extent of the feature; it could die out just outside of the profile limits or it could extend into the Irish Sea; it is currently a complete unknown. Without any other supporting MT data and no other geological or geophysical evidence of its existence it seems unlikely to be a continuation of the feeder zone and more likely to be a large dyke or sill.

The conductive area (2b) between the two granite areas is required by the data as when it was replaced by a resistive area, the fit to the data became much worse. The area is fairly conductive, being around 30-100 Ohm.m, which is more conductive than the Silurian shales seen elsewhere on the models. This could be due to several factors including a fault, a raft of hydrothermally altered country rock or an area of saturated rock. Interestingly, no lower crustal conductor is seen in this profile, unlike the eastern and western profiles, which would suggest that the cause of this conductor is only present underneath the Mourne plutons and doesn't extend to the south.

5. MODEL OF EMPLACEMENT

- A basic magma chamber forms/pools in the same area as the positive gravity anomaly; possibly as Stevenson & Bennett (2011) describe, but it cannot be constrained by this work as the proposed chamber is located off profile. The chamber begins to fractionate as it is cooling with some crustal contamination as reported by McCormick *et al. (*1993) & Meighan *et al.* (1988).
- The first magma travels up the southern feeder zone from the offshore chamber following the local weaknesses in the country rocks; the Silurian sediments strike ENE-WSW with vertical or very steep dips with lots of evidence for faulting and folding of the rocks, making them predominantly weak in this direction, therefore it is easiest for the magma to travel in this direction (Anderson 2004).
- The first sheet is intruded with a thickness of around 4km. This first pulse is the least fractionated or represents the original magma composition. The change in magma flow from vertical to horizontal could be due to several factors as proposed by Cruden (1998) the magma could collide with an active horizontal fracture, a ductile horizon or a unit with high fracture toughness or it could also be due to the magma arriving at a level of neutral buoyancy. The most likely situation in this case is neutral buoyancy or an active horizontal fracture; the country rocks are almost always steeply dipping so the magma is unlikely to encounter a horizontal unit as a barrier to flow. Space creation for this unit occurs by roof uplift and/or deformation of the host rocks.
- As seen in section 4.1 the first, less resistive sheet now lies below the feeder zone and is likely to have moved relatively downwards at some point. The local area has a lot of deformation so the first intrusion of the magma could have caused movement on pre-existing faults. The first magma pulse could also have had longer to cool and if it was composed of over 50% crystals, this would guarantee the rigidity of the body and the next unit would intrude beside it (Vigneresse 2004). Therefore, in this case, the next unit would intrude above, pushing the original unit down; possibly by movement on faults bounding the original unit. This unit would go downwards with the surrounding areas uplifted including the feeder zone. This is similar to a cauldron subsidence model; however, the classic theory of the rocks sinking into the molten or partially molten chamber is not possible in this area as there is no evidence of a chamber below the Mournes outcrops or even anywhere on the profile. This leads to the assumption that it is located off-profile in the vicinity of the gravity anomaly.

Therefore the space for this lower layer must have been created mainly by the uplift of the surrounding country rocks with slight downwards movements of the body, a combination of laccolithic and lopolithic movement. This first sheet is either granite G_1 or a new G_0 granite but there is no way to tell given the available information. It is more likely to be a G0 granitic body as there are outcrops of G_1 granite at the surface which are hard to explain using this theory. Another option would be that a very large original sheet was intruded with the next G_2 granite intruding into the middle, leaving the original G_1 granite above and below. Leaving outcrops of G_1 above G_2 at the surface and the rest of G_1 inferred as the lower resistor in the central eastern block. However you would expect that for G_2 to intrude into the middle of G_1 it would have to be less than 50% crystallised and so the two lithologies would be mixed, which they are not, so this seems less likely. So more likely the new G_0 granite crystallises until stable, the chamber fractionates further and the G_1 granite travels along the same conduit and is intruded above the G_0 granite.

- The chamber fractionates further. The G_2 granite travels along the same conduit and is intruded as a sheet between granite G_0 and granite G_1 or above granite G_1. This second sheet must be larger than the first, extending further to the north. This would explain the granite seen underneath site emc002 between the surface and 1.5km depth which must be accounted for. This model fails to explain the presence of the deeper granites; however, these have been shown (Chapter 4.2) to be fairly unconstrained. A re-testing of this site is needed to confirm their presence at depth.
- Further fractionation of the magma chamber occurs and granite G_3 travels along the same conduit and is intruded in between granite G_0 and granite G_2 or above granite G_2.
- New faults or new weaknesses in the surrounding country rocks cause a new feeder zone to propagate in the west; or a freezing of the eastern conduit. The magma chamber fractionates further and granite G_4 travels as a thin sheet and is intruded as a new western pluton. The space is created by downward movements of the floor. The evidence for this mainly comes from the shape of the pluton with its large rounded pool underneath the surface outcrop with a distinct thin feeder sheet seen to the south. The space is unlikely to be created by roof uplift as the main body extends below the feeder zone suggesting rather a downward movement of the floor, lopolithic movements.

- A new influx of basaltic magma to the chamber causes a return to a composition similar to granite G_1. A more mafic G_5 granite travels along the new western feeder and is intruded as a sheet above granite G_4.
- The western feeder sheet is either faulted during or after the granite emplacement.
- In both plutons the magma flows NNE/SSW in concordance with the AMS data from Stevenson *et al.* (2007) and Stevenson & Bennett (2011).

6. DISCUSSION

The findings of this study suggest that both the Eastern and Western Mourne granitic plutons were emplaced as thin (<6km) tabular sheets. From the magnetotelluric profiles there appears to be no evidence for a ring-dyke around the plutons, a magma chamber underneath the plutons or a "bell-jar" geometry. It is clear that the resistive bodies extend down to 8km in the east and 6km in the west, which are interpreted as the granite lithologies seen at the surface. The southern profile confirms the presence of both these granite bodies in the subsurface to the south of the Mournes.

Although the findings of this study agree with those of Stevenson *et al.* (2007) and Stevenson & Bennett (2011) that the granites were emplaced as tabular sheets; the geometry of the granites have lead to the conclusion that the emplacement was a combination of laccolithic and lopolithic mechanisms rather than solely laccolithic. Their linear flow directions of NNE/SSW also appear to be supported by the southerly dipping granite seen in the eastern profile which is interpreted as the feeder zone for the pluton. This feeder zone can be seen as far as possible to extend down towards the positive Bouguer anomaly as reported by Reay (2004), which was interpreted by Stevenson *et al.* (2007) as a likely location for the magma chamber feeding the Mournes. When the eastern pluton was remapped by Hood (1981) he redefined some of the G_1 roof outcrops, this undermined the cauldron subsidence mechanism and he sought a new explanation for the emplacement. Although discussing many ideas there was a lack of evidence to support any theory other than cauldron subsidence. This study lends further support to his remapped geology and an explanation for its geometry. The western pluton was always considered to have been emplaced with the same cauldron subsidence mechanism with Gibson (1984) and Cooper & Johnston (2004) stating that the present level of erosion allows only the granitic roofs to be seen. This explanation for the lack of 'wall' exposures is now undermined, the western MT profile shows that 'walls' *sensu* the cauldron subsidence model are non-existent and that the intrusion is a thin sheet with a deeper central area underneath the western Mourne pluton. It has long been established that negative Bouguer anomalies are associated with acidic intrusions; Bott (1953) suggests this is due to density contrasts between the surrounding country rocks and the less dense acid intrusions. He considers Bouguer anomalies over granites throughout Britain are Ireland and suggests that whilst most of them are negative, over the Mourne granites there is no anomaly, he concludes this is due to a large basic intrusion below which are represented as positive

anomalies; “Gravity survey over Slieve Gullion, Carlingford, and the Mountains of Mourne show that although the surface outcrop of granophyre and granite predominates, underneath the total mass of basic rock must be at least a hundred times that of the acid rock.” (Bott 1953). This idea, in a sense, has prevailed with the lack of anomaly over the Mournes being attributed to a basic magma chamber underneath the Mournes in the cauldron subsidence theory. In Stevenson *et al’s* (2007) laccolithic theory he also states that the granite sheets must be underlain by some sort of mafic layer that is approximately the same thickness of the granite. Nevertheless, neither of these mafic bodies can be seen on the magnetotelluric profiles. From Bott (1953) it is also apparent that the Silurian shales and greywackes should be denser than the granites if they are analogous to the ones mentioned in his study. Therefore a new explanation of this negative anomaly is needed. It may be related to the mid-crustal conductor seen in the eastern and western profiles, yet, as it is ambiguous as to what these conductors represent this cannot be confirmed in this study.

The Mournes were considered one of the ‘classic’ cauldron subsidence examples; yet the findings of this study have added to the collecting evidence which suggests that this was not the case. The cauldron subsidence model was produced using only outcrop data, yet we now know from Reay’s (2004) gravity data that a positive anomaly is present offshore to the south of the Mournes, from Stevenson *et al’s.* (2007) and Stevenson & Bennett’s (2011) AMS data that the external and internal contacts are gently dipping, and that the plutons contain linear flow directions of NNE/SSW. From this study we have discovered the subsurface geometry of the plutons and the fact that the granites extend to the south in the subsurface. When you consider all of these findings together, alongside the outcrop data, the cauldron subsidence model no longer gives a satisfactory explanation. The findings of this study along with the previous work suggest that the Mourne plutons were emplaced in a combined laccolithic and lopolithic style rather than a cauldron subsidence mechanism. These findings could have implications for granitic plutons worldwide; many of which owe their emplacement models to the cauldron subsidence models first developed in the British and Irish Palaeogene Igneous Province by Clough *et al*. (1909) and Richey (1927) among others.

A limitation of using the MT method in this area is the uncertainty of how the steep topography may have affected the data, it was clear when using the 100 Ohm.m half space during the modelling process that it was having an effect, yet, whether the model accurately represented the topography or whether the topographic effect is actually contained within the data cannot be determined. This topographic effect was assumed to be having a greater effect

on the TE mode (Chapter 3.4) so; this along with the TE mode's sensitivity to 3D effects justifies its lower weighting in the final inversion process. It is clear also that the MT method cannot distinguish between the different granitic lithologies seen at the surface due to their similar resistivities, this leads to an interpretation of their individual locations within the granite bodies rather than fact. Therefore if the individual units could be determined it may give an even better picture or even require a revision of the emplacement mechanism. However, the difference it resistivity between the granites and the country rocks is much larger suggesting that the geometry of the overall bodies is well constrained. Although these profiles are clear on the geometry of the granites in the subsurface, it has to be remembered that other structures could exist outside of these profiles which necessitate a different emplacement mechanism. It is also important to state that these models are imaging only 1D and 2D structures; any 3D structures present in the area would require a 3D inversion and model. This then leads to further research which is needed; a 3D model with a 3D topography DTM (Digital Terrain Model) would further constrain the emplacement mechanism. For this to be achieved more profiles are needed across the area, this will also ensure any other features have been captured. The best location for these profiles would be; a new 20km line across the western pluton parallel to the proposed magma flow direction to give a cross sectional view across the whole system, another ideal line would be one which extends to the area containing the positive gravity anomaly to further constrain what this is and if/how it is connected to the Mournes plutons, alongside this would be a gravity model to help constrain the geometry of the body. An eastwards extension of the SLA line would be useful to further constrain the granites seen at the end of this profile; a new profile to also test the connectivity between the resistors seen at the end of the SLA profile and the EMC profile would also be helpful as the possibility of their concentric continuation cannot be ruled out by the data presented here.

7. CONCLUSIONS

In his book 'The Nature and Origin of Granite' (1997) Pitcher states 'If only we could see under the surface!' when discussing potential emplacement mechanisms for granitic plutons. I believe this study has 'seen' under the surface of the Mournes, if only along three profile lines, and so, has greatly aided the geological understanding of this area. MT surveys could help to decipher plutonic emplacement worldwide by 'looking underneath the surface'.

The data presented here show that the subsurface structures underneath both the western and eastern plutons are thin (<6km), granitic sheets rather than large, 'bell-jar' geometries extending down to around 10km depth. These findings, alongside no other evidence for a ring-dyke or a magma chamber directly below the Mournes, undermine the theory for a cauldron subsidence emplacement mechanism. They instead advocate a combined laccolithic and lopolithic emplacement mechanism where the laccolithic (roof uplift) methods dominate.

ACKNOWLEDGEMENTS. I would like to thank many people for their help and assistance in making this possible; firstly The Geological Survey of Northern Ireland and The Natural Environmental Research Council for giving us the funding which made this study possible. Thanks go to The Geological Survey of Northern Ireland (GSNI) for also providing logistical support and additional geophysical data, with special thanks to Derek Reay for giving additional data, help, advice, support and field assistance. Special thanks to Mohammed Dessisa also of GSNI for his MT advice and support in the field. Thanks also to Orla Gallagher and Claire McGinn (GSNI) for site permitting. A huge thanks goes to The Dublin Institute of Advanced Studies (DIAS) for providing MT field equipment, MT field training and assistance, help and training with data editing, modelling and the provision of software. A very big thank you to Dr. Mark Muller (DIAS) for his endless help, advice and support without which the project would not have been possible, thanks also for his comments which much improved the manuscript. Thanks also to Colin Hogg (DIAS) and Maryam Hussain (Formerly DIAS) for field assistance and help, and to Alan Jones among others at DIAS for MT support and making our time in Ireland much more interesting! The Mourne Heritage Trust (John McAvoy and Dave Farnan) and the Mourne Trustees, The Forestry Service, Northern Ireland Water, The National Trust and all the local farmers who gave us access to their lands/fields are also thanked. Ciaran Chittock and Siobhan Austin (Methodist College, Belfast) and Tom Henderson (University of Plymouth) are also thanked for their field assistance. Last, but by no means least I would like to thank Chris Yeomans and Dr. Carl

Stevenson. Chris, for his help and company in the field, for the many discussions about our projects and for editing and modelling half of our data. Dr. Carl Stevenson for his help, guidance and informative discussions throughout all stages of the project, without which, the project would not have been successful.

8. REFERENCES

Anderson, E.M., (1936). Dynamics of the Formation of Cone-sheets, Ring-dykes and Cauldron Subsidences. *The Proceedings of the Royal Society of Edinburgh*, **56**, p.128-157.

Anderson, T.B., 2004. Southern Uplands-Down-Longford Terrane. In Mitchell, W.I. *The Geology of Northern Ireland, Our Natural Foundation*. Belfast: Geological Survey of Northern Ireland. p. 41-60.

Bott, M.H.P., (1953). Negative Gravity Anomalies over Acid "Intrusions "and their Relation to the Structure of the Earth's Crust. *Geological Magazine*, **90(4)**, p.257-267.

Bunger, A.P. & Cruden, A.R., (2011). Modeling the growth of laccoliths and large mafic sills: Role of magma body forces. *Journal of Geophysical Research*, **116**, p.1-18.

Clough, C.T., Maufe, H.B. & Bailey, E.B., (1909). The Cauldron-subsidence of Glen Coe and the associated igneous phenomena. *The Quaterly Journal of the Geological Society*, **65**, p.611-678.

Cooper, M.R. & Johnston, T.P., 2004. Late Palaeozoic Intrusives. In Mitchell, W.I. *The Geology of Northern Ireland, Our Natural Foundation*. Belfast: The Geological Survey of Northern Ireland. p. 61-68.

Cooper, M.R. & Johnston, T.P., 2004. Palaeogene Intrusive Igneous Rocks. In Mitchell, W.I. ed. *The Geology of Northern Ireland*. 2nd ed.: Geological Survey of Northern Ireland. Ch. 15. p. 179-198.

Cruden, A.R., (1998). On the emplacement of tabular granites. *Journal of the Geological Society, London*, **155**, p.853-862.

Gamble, J.A., Wysoczanski, R.J. & Meighan, I.G., (1999). Constraints on the age of the British Tertiary Volcanic Province from ion microprobe U-Pb (SHRIMP) ages for acid igneous rocks from NE Ireland. *Journal of the Geological Society*, **156**, p.291-299.

Gibson, D., (1984). The petrology and geochemistry of the western Mourne granites, Co. Down, N. Ireland. *Unpublished PhD thesis, Queens University Belfast*.

Groom, R.W. & Bailey, R.C., (1989). Decomposition of Magnetotelluric Impedance Tensors in the Presence of Local Three-Dimensional Galvanic Distortion. *Journal of Geophysical Research*, **94(B2)**, p.1913-1925.

Hood, D.N., (1981). Geochemical, petrological and structural studies on the Tertiary granites and associated rocks of the Eastern Mournes Mountains, Co. Down, Northern Ireland. *Unpublished PhD thesis, Queens University Belfast*.

Horsman, E., Morgan, S., de Saint-Blanquat, M., Habert, G., Nugent, A., Hunter, R.A. & Tikoff, B., (2010). Emplacement and assembly of shallow intrusions from multiple magma pulses, Henry Mountains, Utah. *Earth and Environmental Science Transactions of the Royal Society of Edinburgh*, **100(Sp Iss 1-2)**, p.117-132.

Hutton, D.H.W., (2009). Insights into magmatism in volcanic margins: bridge structures and a new mechanism of basic sill emplacement – Theron Mountains, Antarctica. *Petroleum Geoscience*, **15**, p.269-278.

McCormick, A.G., Fallick, A.E., Harmon, R.S., Meighan, I.G. & Gibson, D., (1993). Oxygen and Hydrogen Isotope Geochemistry of the Mourne Mountains Tertiary Granites, Northern Ireland. *Journal of Petrology*, **34(6)**, p.1177-1202.

McNeice, G.W. & Jones, A.G., (2001). Multisite, multifrequency tensor decomposition of magnetotelluric data. *Geophysics*, **66(1)**, p.158-173.

McNulty, B.A., Tobisch, O.T., Cruden, A.R. & Gilder, S., (2000). Multistage emplacement of the Mount Givens pluton, central Sierra Nevada batholith, California. *The Geological Society of America*, **112**, p.119-135.

Meighan, I.G., Gibson, D. & Hood, D.N., (1984). Some aspects of Tertiary acid magmatism in NE Ireland. *Mineralogical Magazine*, **48**, p.351-363.

Meighan, I.G., McCormick, A.G., Gibson, D., Gamble, J.A. & Graham, I.J., (1988). Rb-Sr isotopic determinations and the timing of Tertiary central complex magmatism in NE Ireland. *The Geological Society of London Special Publications*, **39**, p.349-360.

Olona, J., Pulgar, J.A., Fernández-Viejo, G., López-Fernández, C. & González-Cortina, J.M., (2010). Weathering variations in a granitic massif and related geotechinal properties through seismic and electrical resistivity methods. *Near Surface Geophysics*, **8**, p.585-599.

Petford, N., Cruden, A.R., McCaffrey, K.J.W. & Vigneresse, J.-L., (2000). Granite magma formation, transport and emplacement in the Earth's crust. *Nature*, **408**, p.669-673.

Pitcher, W.S., 1997. *The Nature and Origin of Granite*. 2nd ed. London: Chapman and Hall.

Reay, D.M., 2004. Geophysics and Concealed Geology. In Mitchell, W.I. *The Geology of Northern Ireland, Our Natural Foundation*. Belfast: The Geological Survey of Northern Ireland. p. 227-248.

Richey, J.E., (1927). The structural relations of the Mourne Granites. *Quaternary Journal of the Geological Society*, **83**, p.653-688.

Robbie, J.A., (1955). The Slieve Binnian Tunnel, an aqueduct in the Mourne Mountains, Co. Down. *The Bulletin of the Geological Survey of Great Britain*, **8**, p.1-20.

Simpson, F. & Bahr, K., 2005. *Practical Magnetotellurics*.: Cambridge University Press.

Stevenson, C.T.E. & Bennett, N., (2011). The emplacement of the Palaeogene Mourne Granite Centres, Northern Ireland: new results from the Western Mourne Centre. *Journal of the Geological Society, London*, **168**, p.1-6.

Stevenson, C.T.E., Owens, W.H., Hutton, D.H.W., Hood, D.N. & Meighan, I.G., (2007). Laccolithic, as opposed to cauldron subsidence, emplacement of the Eastern Mourne pluton, N. Ireland: evidence from anisotropy of magnetic susceptibility. *Journal of the Geological Society*, **164**, p.99-110.

Taylor, H.P. & Sheppard, S.M.F., 1986. Igneous rocks: I. Processes of isotopic fractionation and isotope systematics. In Valley, J.W., Taylor, H.P. & O'Neil, J.R. *Stable Isotopes in High Temperature Geological Processes*. p. 227-271.

Thompson, P., Musett, A.E. & Dagley, P., (1987). Revised *°Ar/39Ar age for the granites of the Mourne Mountains, Ireland. *Scottish Journal of Geology*, **23**, p.226-230.

Vigneresse, J.L., (2004). A new paradigm for granite generation. *Transactions of the Royal Society of Edinburgh: Earth Sciences*, **95**, p.11-22.

Yeomans, C., 2011. *Geothermal implications of the Mourne Mountains: constraints from magnetotelluric modelling*. Unpublished MSci Thesis. The University of Birmingham

APPENDIX

1. MT data collection sheets from the fieldwork. (On paper)
2. Tipper and polar diagrams. (On paper)
3. A full collection of strike analysis plots and print outs. (Disc)
4. Full robustness test images and spreadsheet data for the EMC and SLA profile lines. (Disc)
5. Full robustness test images and spreadsheet data for the WMC profile, Yeomans (2011). (Disc)

9.